Determining effective permeability at reservoir scale: Numerical simulations and critical path analysis

by

Barnabas Adeyemi

B.S., University of Lagos, 2016

A THESIS

submitted in partial fulfillment of the requirements for the degree

MASTER OF SCIENCE

Department of Geology
College of Arts and Sciences

KANSAS STATE UNIVERSITY
Manhattan, Kansas

2021

Approved by:

Major Professor
Dr. Behzad Ghanbarian

Copyright

Abstract

Determining the effective permeability (k_{eff}) of geological formations has broad applications to site remediation, aquifer discharge or recharge, hydrocarbon production, and enhanced oil recovery. However, due to the presence of heterogeneity across scales, accurate calculation of k_{eff} requires precise characterization of reservoirs. In the literature, stochastic, theoretical, and numerical methods have been proposed to determine the value of k_{eff}. In this study, we propose applications from critical path analysis (CPA), an upscaling technique from statistical physics. More specifically, we postulate that permeability at the mode of permeability probability function should represent the effective permeability of a reservoir. To validate this hypothesis, we construct two- and three-dimensional random (uncorrelated) geologic formations based on permeability measurements from the Borden site and assume that the permeability distribution conforms to the log-normal probability density function. The log-normal distribution with different geometric means ($4.5\times10^{-12}\leq k_g \leq 1.0\times10^{9}$ m^2) and standard deviations ($0.05\leq \sigma \leq 6$) is used to generate 10 different formations. We apply the COMSOL platform to numerically simulate 2 and 3D flow and determine the k_{eff} in such formations. We also calculate the k_{eff} using several other approaches proposed in the literature, such as perturbation theory, renormalization group theory, and effective-medium approximation. Comparing the numerically determined k_{eff} values with the theoretically estimated ones demonstrates that the CPA provides accurate estimations in both two and three dimensions. Although the CPA estimates the k_{eff} with RMSLE = 0.50 more accurate than the other approaches in two dimensions, the renormalization group theory with RMSLE = 0.90 provides slightly better estimations than the CPA with RMSLE = 1.14 in three dimensions. Results show that although perturbation theory and the

effective-medium approximation provide reasonable k_{eff} estimations in formations with $\sigma < 2$, they substantially overestimate the effective permeability in highly heterogeneous formations. We found that CPA provided a powerful platform to estimate effective permeability at the reservoir scale in uncorrelated formations. However, further investigations are still required to evaluate its predictability in formations with spatial correlations.

Keywords: Critical path analysis, Effective permeability, Log-normal permeability distribution, Spatial heterogeneity, Upscaling

Table of Contents

List of Figures

List of Tables

Acknowledgements

I Thank GOD the Father, My Lord JESUS CHRIST, and My Comforter the HOLY SPIRIT; to Them I owe everything: life, health, and provisions. All the Glory for the success of my program here at Kansas State University belongs to Them.

I am indebted to my Dad, Mr. Samuel Adeyemi, my Mom, Mrs. Florence Adeyemi, and my brothers Emmanuel Adeyemi and John Adeyemi. I want to sincerely express my gratitude to my parents for all they have done for me since day one on earth; Thank you for the upbringing, guiding, and teachings.

I am grateful to my major professor, Dr. Behzad Ghanbarian, for his mentorship and support over the past two years. It would have been utterly impossible to perform this research, needless to mention obtaining meaningful and desired results, without his helpful inputs, feedback and guidance on the work from the start to finish. He has been very helpful since my first day in Manhattan, saving me the trouble of finding my way around the city by picking me up at the airport. He financially supported me during the summer of 2020, when COVID-19 was raging and the economy was under a lockdown. I also want to thank him for writing recommendation letters for my PhD and scholarship applications.

I want to appreciate the vital contributions of my thesis advisory committee members: Dr. Claudia Adam and Dr. Larry Winter for their extremely helpful feedback and comments that have all helped to shape this thesis document into what it is today. Their inputs since the start of this research, through the proposal defense, up till this very moment have been consistently useful.

I also appreciate every member of the porous media research lab: Misagh, Brandon, and Alireza for friendship and companionship during these two years. What a wonderful experience

to meet these great individuals, and I am truly thankful that I learned about their cultural backgrounds, which are starkly different than mine, and glimpsed a view of life in other parts of the world.

I owe a debt of gratitude to the Department of Geology for support through graduate teaching assistantships and scholarships. Indeed, affording education and a life in Manhattan would have been impossible for me without this generous and magnanimous financial support package by the department. It has been a great honor to work as a graduate teaching assistant at the department for two years. I am very grateful to the department head, Dr. Pamela Kempton, for her assistance and support all through my program; for helpful feedbacks and revisions on thesis proposal and thesis documents, and very importantly, for writing recommendation letters for my PhD and scholarship applications.

To every faculty member in the department and every professor at Kansas State University that I attended their classes, I say a big Thank you for your time. I want to express my gratitude to Dr. Abdelmoneam Raef for his help and support during my education in the department, advice during the difficult times, and recommendation letters for PhD applications. I am also grateful to Dr. Aida Farough for all her advice and assistance with my teaching duties and also with recommendation letters for PhD applications. It has been a wonderful learning experience here at the Department of Geology in Kansas State University.

I would like to appreciate the National Association of Black Geoscientists and the Kansas Geological Foundation for support through scholarships in the Fall 2020 semester, which really helped in covering costs during my program.

Lastly, I want to sincerely thank everyone that I've come across during my time here at Kansas State University. This includes every faculty member, graduate teaching assistant graduate and undergraduate student. Thank you!

Chapter 1 - Introduction

1.1. Background

Investigating flow and transport in geological formations, such as aquifers and reservoirs, is essential in numerous areas of geology and engineering: for CO_2 sequestration, site remediation, groundwater hydrology, and enhanced oil recovery. Under fully saturated conditions, one key parameter is effective permeability (k_{eff}), which indicates the overall capability of a formation to allow the passage of fluid through it. Geological formations are heterogeneous and typically composed of zones of various materials with different permeabilities spanning several orders of magnitude (Freeze and Cherry, 1979; Akpoji and De Smedt, 1993; Oladele et al., 2019). Experimental studies (Bjerg et al., 1992; Rehfeld et al., 1992; Sudicky, 1986) show that the histogram of permeability values measured on core samples approximately follows the log-normal probability density function. In fact, the log-normal permeability distribution has been widely used to study flow and transport at large scales (Colecchio et al., 2020; Edery et al., 2014; Hristopulos, 2003; Zarlenga et al., 2018). This means the spatial heterogeneity of a formation can be captured by truncated log-normal distribution parameters, i.e., mean and standard deviation as well as its lower and upper cutoffs.

An active subject of research in geosciences has been determining the effective value of permeability (Dagan, 1993; Masihi et al., 2016; Rasaei and Sahimi, 2009). Various techniques, including theoretical and numerical methods, have been proposed to calculate the value of k_{eff} in geological formations (Renard and de Marsily, 1997; Sanchez-Vila et al., 2006). Although numerical methods are suitable for any type of aquifers and reservoirs, they are computationally demanding, particularly for three-dimensional (3D) simulations. As a result, theoretical models have been frequently utilized for the estimation of k_{eff}.

These models include the simple averaging techniques (Deutsch, 1989), perturbation theory (Stepanyants and Teodorovich, 2003), self-consistent approximation (Dagan, 1979), effective medium approximation (Fokker, 2001), renormalization group theory (King, 1989), wavelet transformation (Rasaei and Sahimi, 2009), and information theory (Wood and Taghizadeh, 2020). As most of the models applied to the estimation of k_{eff} are based on perturbative methods (Sanchez-Vila et al., 2006), we will briefly review several perturbation theory-based models used in the hydrology literature in what follows.

1.2. Perturbative models

Within the framework of perturbation theory, the pressure head in the Darcy equation is first expanded in a power series in terms of permeability fluctuations (Sanchez-Villa et al., 2006) after which a solution for velocity is constructed by the application of Darcy's law (Sanchez-Villa et al., 2006; Renard and de Marsily, 1997; Stepanyants and Teodorovich, 2003). Using these methods, Matheron (1967) and Gutjahr (1978) proved that the quantities of the equation popularly known in hydrogeology as Matheron's conjecture are the first two terms of the Taylor series expansion of an exponential function. Although not sufficiently proven to be exact in 3D flow, the conjecture is known to give the effective permeability in log-normally distributed permeability fields as the harmonic mean (k_{eff}=k_{h}) in one-dimensional (1D) flow and geometric mean (k_{eff}=k_{g}) in two-dimensional (2D) flow (De Wit, 1995). Gelhar and Axness (1983) also used a perturbation theory-based approach to derive expressions to link the effective permeability to the variance σ^2 in the case of a log-normally distributed anisotropic medium with arbitrary orientation of the stratification. Later, Dagan (1993) extended their result for log-normal permeability fields through the σ^4 order.

Indelman and Abramovich (1994) proved that the k_{eff} expression through order σ^4 for an anisotropic permeability field depends not only on the anisotropic ratios, variance, and space dimensions but also on the shape of the permeability distribution function. Importantly, their work highlighted major inconsistencies in Matheron's conjecture for anisotropic and 3D permeability systems. Their expression, which we denote here as the anisotropic perturbation theory (ANPT), is given below:

$$k_{\text{eff}}(i) = k_g \left\{ 1 + \left(\frac{1}{2} - \alpha_i\right)\sigma_Y^2 + \frac{1}{2}\left[\left(\frac{1}{2} - \alpha_i\right)^2 + \gamma_i\right]\sigma_Y^4 \right\} \quad (1)$$

where σ_Y is the standard deviation of the natural logarithm of the permeability (Y = ln(k)), i indicates the principal hydraulic conductivity direction (i =1,2,3 in three dimensions), and $\alpha_1 = \alpha_2 = (1-\chi)/2$ and $\alpha_3 = \chi$. χ depends on the anisotropic ratio of the permeability field and γ_i depends on the permeability correlation function. In the case of isotropy, χ = 1/3 and $\gamma_i = 0$.

With the aim of further proving the dependence of the k_{eff} expression on the permeability distribution function, De Wit (1995) derived the terms for the k_{eff} expression up to the order σ_Y^6. His work exposed some of the underlying inaccuracies of Matheron's conjecture as the σ_Y^6 order terms of his derivation contained parameters and factors that are not available in the σ_Y^6 order terms of Matheron's conjecture expansion. The expression, here referred to as the simple perturbation theory (SPT), is:

$$k_{\text{eff}} = k_g \left[1 + \left(\frac{1}{2} - \frac{1}{d}\right)\sigma_Y^2 + \frac{1}{2}\left(\frac{1}{2} - \frac{1}{d}\right)^2 \frac{\sigma_Y^4}{2} + \left(\frac{1}{2} - \frac{1}{d}\right)^3 \frac{\sigma_Y^6}{2} + \varepsilon \right] \quad (2)$$

where ε is a term that depends on the permeability distribution function and vanishes for *d* (formation dimension) = 1 and 2. For three-dimensional flow, however, it was numerically found that ε is approximately equal to $-0.0014\sigma_Y^6$ for a Gaussian log permeability field (De Wit, 1995; Sanchez-Villa, 2006).

More recently, Stepanyants and Teodorovich (2003) used a different perturbative approach for constructing a perturbation series to calculate effective permeability. Rather than applying perturbation expansions to pressure head or variance as in earlier works, they performed their expansions on velocity and used Feynman diagrams for the derivation of terms of perturbative series. Their approach led to a solution presented in the form of a power series for the inverse coefficient of permeability, which we refer to as the alternative perturbation theory (ALPT) and is given by

$$k_{\text{eff}} = k_g \exp\left(-\frac{\sigma_Y^2}{2}\right)\left[1 - \frac{d-1}{d}\sigma_Y^2 + \frac{1}{2}\left(\frac{d-1}{d}\right)^2 \sigma_Y^4\right]^{-1} \quad (3)$$

Although the derivation of most perturbative models requires advanced mathematical and computational skills, the inability of these methods to accurately estimate k_{eff} in heterogeneous formations where permeability fluctuations become very large (King, 1989; Sanchez-Villa et al., 2006; Dagan et al., 2013) is well known in the literature.

Numerical simulations of Dykaar and Kitanidis (1992) as well as the renormalization calculations of Attinger et al. (2002) seemed to confirm the validity of Matheron's conjecture for multi-Gaussian permeability fields with σ_Y^2 as large as 7. However, accurate numerical simulations by Jankovic et al. (2003A; 2003B) showed that the well-known self-consistent approximation (see e.g., Dagan, 1989) led to excellent agreement with numerical results while Matheron's conjecture largely overestimated k_{eff} for $\sigma_Y^2 > 1$ in a medium made of a dense ensemble of inclusions of independent log-normal k. De Wit (1995) also showed that the SPT, and most perturbative methods, estimates k_{eff} with an error less than 1% when $\sigma_Y < 1.7$ for the Gaussian distribution of k and $\sigma_Y < 2$ for the exponential k distribution. In another study, Sarris and Paleologos (2004) showed that there is good agreement between k_{eff} Monte Carlo simulation results and ANPT estimations for $\sigma_Y^2 < 2$.

Such results demonstrate the inability of perturbative methods to accurately estimate the effective permeability in statistically heterogeneous formations. Consequently, we propose a powerful technique for estimating effective permeability and apply it to ten different uncorrelated formations. We also show its reliability by comparing its estimations to other model estimations (including the perturbative methods described here) in this study.

1.3. Objectives

Critical path analysis (CPA) is a promising upscaling technique from statistical physics. Although CPA has been widely applied to estimate k_{eff} at the core scale (Ghanbarian, 2020; Ghanbarian et al., 2016; Katz and Thompson, 1986), to the best of our knowledge its applications to the reservoir scale are very limited (Hunt and Idriss, 2009). Therefore, the objectives of this project are to: (1) develop a novel approach for applying the concept of CPA to the estimation of effective permeability at the reservoir scale, and (2) evaluate the performance of the CPA approach by comparing effective permeability estimated by CPA with that determined by numerical simulations, and (3) compare the accuracy of the CPA to other theoretic models, such as perturbation theory, the effective-medium approximation, and renormalization group theory. To achieve our objectives, the proposed research focuses on a wide range of aquifers/reservoirs with different levels of heterogeneity. In the next chapter, we briefly describe the critical path analysis, renormalization group theory, and the effective-medium approximation.

Chapter 2 - Theory

2.1. Critical path analysis

CPA was originally proposed in the physics literature to scale up conductivity in random (uncorrelated) and heterogeneous systems with large fluctuations in local conductivity (Ambegaokar et al., 1971; Pollak, 1972). Based on the CPA, fluid flow in a heterogeneous formation with a broad distribution of permeabilities is controlled by permeabilities whose magnitudes are greater than some critical permeability (Hunt, 2001). In other words, transport is dominated by high-permeability zones, while low-permeability ones have trivial contribution to the overall transport (Hunt et al., 2014).

Imagine a reservoir constructed of grid blocks of various permeabilities. To calculate the value of critical permeability, we should first remove all the grid blocks from the reservoir. We then replace them in their original locations in a decreasing order from the largest to the smallest permeability. As the first largest permeabilities are replaced, there is still no percolating cluster. However, after a sufficiently large fraction of grid blocks is replaced within the reservoir, a sample-spanning cluster forms and the system starts percolating. The critical permeability is defined as the smallest permeability required to form a conducting sample-spanning cluster. Fluid flow and transport take place through the sample-spanning cluster which is composed of two components: (1) the dead-end part that does not contribute to flow, and (2) the backbone, the multiply-connected part of the cluster, through which fluid flow occurs. The grid blocks in the backbone can be divided to two groups: (i) those in the blobs that are multiply connected and make flow paths very tortuous, and (ii) those that would split the backbone into two parts, if removed, that are called red grid blocks (Pike and Stanley, 1981).

At the core scale, Katz and Thompson (1986) argued that the effective permeability is controlled by the critical pore-throat radius corresponding to the mode of the probability density function of pore throats. Analogously, we postulate that critical permeability corresponding to the mode of permeability distribution should represent the effective permeability (k_{eff}) of a formation. An example of how this concept can applied at the reservoir scale (to the permeability distribution of a formation) is shown in Figure 2-1.

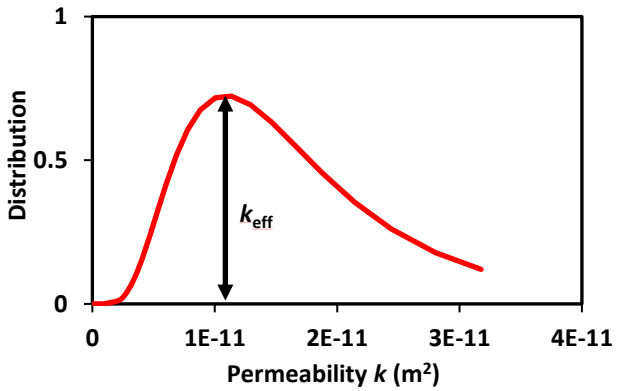

Figure 2-1. Application of the CPA approach to estimate k_{eff} in geological formations

2.2. Renormalization group theory

Renormalization group theory (RGT) is another powerful upscaling technique from statistical physics (Reynolds et al., 1977; Stinchcombe and Watson, 1976). Using the analogy between fluid flow through a porous medium and flow of current through an electric circuit, King (1989) mapped a block of cells of different permeabilities into an equivalent resistor network and ultimately to a single resistor. Using this terminology, the effective permeability of a 2×2 block of isotropic cells was obtained in two dimensions as follows (King, 1989):

$$k_{\text{eff 2D}} = \frac{4(k_1+k_3)(k_2+k_4)[k_2k_4(k_1+k_3)+k_1k_3(k_2+k_4)]}{[k_2k_4(k_1+k_3)+k_1k_3(k_2+k_4)][k_1+k_2+k_3+k_4]+3(k_1+k_2)(k_3+k_4)(k_1+k_3)(k_2+k_4)} \quad (4)$$

where k_1, k_2, k_3, k_4 are permeability values of neighbouring cells used in the 2D renormalization.

In three dimensions, the process of renormalization is more complicated. The fundamental structure is a $2 \times 2 \times 2$ cube, with uniform pressure on two parallel faces and no flow boundary conditions on the remaining four faces. Several transformations must be performed in order to obtain an equivalent resistance. Green and Patterson (2007) used the idea of splitting a $2 \times 2 \times 2$ cube into four components, treated each as a two-dimensional block and calculated the effective permeability as follows (Green and Paterson, 2007):

$$k_{\text{eff 3D}}(k_1, k_2, k_3, k_4, k_5, k_6, k_7, k_8) = \frac{1}{4}[k_{\text{eff 2D}}(k_1, k_2, k_3, k_4) + k_{\text{eff 2D}}(k_5, k_6, k_7, k_8) + k_{\text{eff 2D}}(k_5, k_6, k_1, k_2) + k_{\text{eff 2D}}(k_7, k_8, k_3, k_4)] \quad (5)$$

2.3. Effective medium approximation

In the effective medium approximation (EMA), developed by Kirkpatrick (1973), a heterogeneous formation is replaced by a homogeneous one of permeability k_{eff}, which is the same as the permeability of the actual heterogeneous formation. The spatial dependence of permeability in the heterogeneous formation results in local perturbations about the effective permeability of the homogeneous formation. The effective permeability can then be calculated by setting the average perturbation to be zero (Kirkpatrick, 1973)

$$\int \frac{k - k_{\text{eff}}}{k + \left(\frac{z}{2} - 1\right)k_{\text{eff}}} f(k)dk = 0 \quad (6)$$

where $f(k)$ is the probability density function of permeability, and z is the coordination number equal to 4 and 6 respectively in two and three dimensions. We should note that Eq. (6) with $z = 4$ in two dimensions and 6 in three dimensions reduces to the self-consistent approximation.

Chapter 3 - Materials and Methods

3.1. Heterogeneity due to spatial variation in permeability

In geological formations and reservoirs, permeability spatially varies. Measurements on cores sampled at different locations in geologic formations from various studies indicate that permeability measurements should approximately conform to the log-normal distribution (Haneberg, 2012; Wainwright and Mulligan, 2013)

$$f(k) = \frac{1}{\sqrt{2\pi}\sigma k} exp\left[-\left(\frac{\ln(\frac{k}{k_g})}{\sqrt{2}\sigma}\right)^2\right], \quad k_{min} \le k \le k_{max} \tag{7}$$

where σ is the standard deviation, and k_{min} and k_{max} are the minimum and maximum permeability values in the formation, respectively. According to Fogg (2010), σ^2 value can be as large as 10 to 15 in natural geological formations.

In Figure 3-1, we show Eq. (7) and its fit to permeability measurements from the Borden site (Sudicky, 1986).

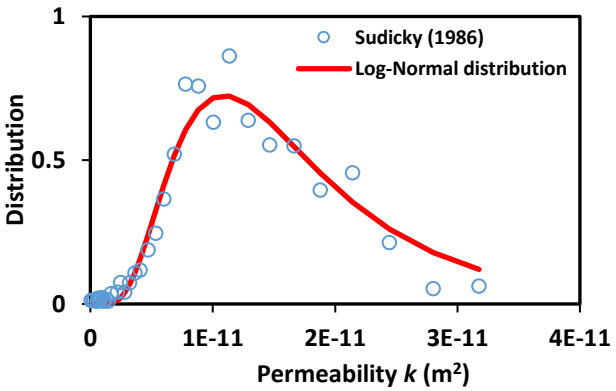

Figure 3-1. The log-normal distribution, Eq. (8), with $\boldsymbol{k_g}$ = 1.5×10^{-11} m^2, σ = 0.56, k_{min} = 6.1×10^{-14} m^2, and k_{max} = 3.2×10^{-11} m^2 fitted with R^2 = 0.80 to the permeability histogram. Permeability measurements are from the Borden site (Sudicky, 1986).

As can be seen, the log-normal distribution with $k_g = 1.5 \times 10^{-11}\text{m}^2$, $\sigma = 0.56$, k_{min} = 6.1×10^{-14} m^2, and k_{max} = 3.2×10^{-11} m^2 characterize the permeability histogram reasonably well with R^2 = 0.80. Based on the results shown in Figure 3-1, we designed nine other formations using the same truncated log-normal distribution but different values of k_g and σ as reported in Table 3.1 and shown in Appendix A.

Table 3.1. Ten different geological formations constructed in this study. k_g is the geometric mean and σ is the standard deviation from the log-normal permeability distribution. k_{min} and k_{max} are the minimum and maximum permeability values in each formation. $(\ln k)_{avg}$ is the average of the natural logarithm of permeability and σ_Y is the standard deviation of the log-transformed permeability distribution ($Y = \ln(k)$). k_{eff} represents the effective permeability simulated by COMSOL in two and three dimensions.

Formation	k_g**(m^2)**	σ	k_{min}/k_{max}	$(\ln k)_{avg}$	σ_Y	k_{eff} **(m^2) (2D)**	k_{eff} **(m^2) (3D)**
1	1.5×10^{-11}	0.56	$6.1\times10^{-14}/3.2\times10^{-11}$	-25.24	0.56	1.05×10^{-11}	1.12×10^{-11}
2	1.5×10^{-12}	0.56	$6.1\times10^{-14}/3.2\times10^{-11}$	-27.54	0.56	1.11×10^{-12}	1.16×10^{-12}
3	1.9×10^{-11}	0.25	$6.1\times10^{-14}/3.2\times10^{-11}$	-24.76	0.25	1.73×10^{-11}	1.76×10^{-11}
4	4.5×10^{-12}	0.40	$6.1\times10^{-14}/3.2\times10^{-11}$	-26.29	0.40	3.92×10^{-12}	4.02×10^{-12}
5	2.6×10^{-11}	0.05	$6.1\times10^{-14}/3.2\times10^{-11}$	-24.37	0.05	2.62×10^{-11}	2.61×10^{-11}
6	5.0×10^{-11}	2.0	$6.1\times10^{-14}/3.2\times10^{-5}$	-27.72	2.0	1.26×10^{-12}	2.28×10^{-12}
7	1.0×10^{-6}	3.0	$6.1\times10^{-14}/3.2\times10^{-5}$	-22.81	3.0	1.67×10^{-10}	5.13×10^{-10}
8	1.0×10^{-3}	4.0	$6.1\times10^{-14}/3.2\times10^{-5}$	-22.9	4.0	2.03×10^{-10}	1.20×10^{-09}
9	1.0×10^{3}	5.0	$6.1\times10^{-14}/3.2\times10^{-5}$	-18.10	5.0	1.46×10^{-08}	1.09×10^{-07}
10	1.0×10^{9}	6.0	$6.1\times10^{-14}/3.2\times10^{-5}$	-15.25	6.0	5.81×10^{-8}	3.94×10^{-07}

Formation 1 is based on the actual measurements from Sudicky (1986) with $k_g = 1.5 \times 10^{-11} m^2$ and $\sigma = 0.56$ as presented in Figure 3-1. Formation 2 is similar to Formation 1, however, its k_g value is one order of magnitude smaller. All other formations were designed so that a wide range of k_g, σ and k_{min}/k_{max} values can be examined. As can be deduced from Table 3.1, k_g and σ values span nearly 21 and 2 orders of magnitude, respectively, covering a wide range of formations with various levels of heterogeneity. Furthermore, the k_{min}/k_{max} ratio is $6.1\times10^{-14}/3.2\times10^{-11}$ in Formations 1 to 5, while $6.1\times10^{-14}/3.2\times10^{-5}$ in Formations 6 to 10, which indicates broader permeability distributions and, thus, higher levels of heterogeneity in the latter.

3.2. Numerical simulations via COMSOL

COMSOL provides a powerful computational platform for simulations of flow and transport. The Multiphysics package of COMSOL is capable of generating both two- and three-dimensional geometries on which the simulations can be performed. Figure 3-2 shows a 3D domain composed of cells of the same size, where the number of cells along each side of the domain represents the domain size. For example, Figure 3-2a plan shows a domain size of 20.

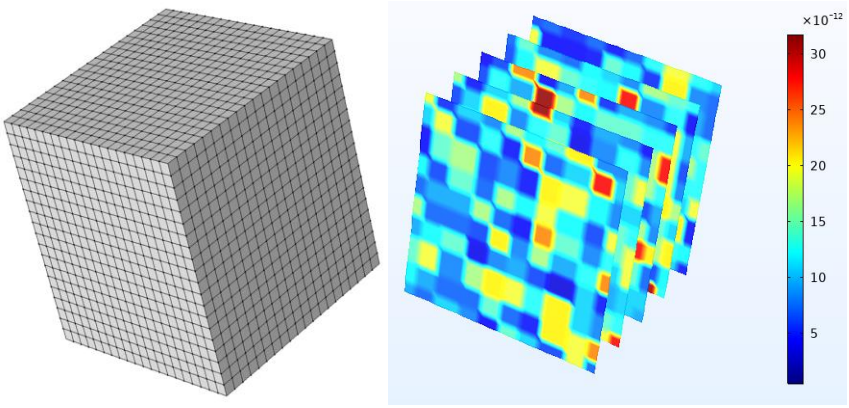

Figure 3-2. (a) A 3D domain of size of 10 m with 20 cells along each side (domain size = 20), and (b) random spatial distribution of permeability values in the same domain.

It is well documented in the literature that numerical simulations are scale-dependent (Sahimi, 2011), which means that the numerically simulated permeability is expected to vary with the domain size. Accordingly, the fluid flow simulations need to be carried out at various domain sizes to find the representative elementary volume (REV), the smallest domain size above which the effective permeability does not vary with size. There exist two approaches to study the scale dependence of permeability: (1) fixing the domain size and decreasing the cell size, or (2) increasing the domain size by increasing the cell size. In the former, the number of cell increases while in the latter the number of cells does not vary. In this study, we applied the first approach. For the 2 and 3D simulations of flow, respectively, square and cubic domains of length 10 m were created. The physical length of 10 m is arbitrary, and any other value can be used without affecting our simulations and results. Each cell in the domain was then randomly assigned a specific value of permeability from the log-normal probability density function. Fig. 3-2b presents the spatial distribution of permeability for the same domain depicted in the same figure. We should point out that our focus is on geologic formations with an uncorrelated distribution of permeability.

Flow was simulated through the 2- and 3-D formations by COMSOL, which solves the pressure form of Darcy's law together with the mass conservation equation. For all the simulations, hydraulic head boundary conditions were applied along the flow direction with no-flow conditions applied in the perpendicular directions. The hydraulic head was set equal to 2 m at one side of the flow direction and to 0 at the other side, while the dynamic viscosity and the water density were set equal to $8.9 \times 10^{-4}\ Pa.s$ and $1000\ kg/m^3$, respectively.

To find the REV, different domain sizes were used. At each domain size, the effective permeability was computed by running simulations 60 times and then averaging over all the

iterations to remove the bias in the simulations. The effective permeability was plotted against the domain size to determine the k_{eff} above the REV.

3.3. Estimating k_{eff} via theoretical models

In this study, we evaluate several theoretic models for estimating effective permeability by applying them to the permeability distributions corresponding to 10 different formations with different levels of heterogeneity (Table 3.1). To estimate the k_{eff} via the perturbative methods i.e., ANPT, Eq. (1), SPT, Eq. (2), and ALPT, Eq. (3), we used the log-normal permeability distribution parameters given in Table 1. For the ANPT model, we set χ = 1/3 and γ_i = 0 for isotropic formations as described by Sanchez-Villa et al. (2006) and Indelman and Abramovich (1994).

To estimate the k_{eff} using the CPA, we determined the value of permeability corresponding to the mode of the log-normal permeability distribution by the following expression: $k_{\text{eff}} = \exp\left[\ln\left(k_{\text{g}}\right) - \sigma^2\right]$.

For the RGT, we constructed two- and three-dimensional matrices in MATLAB whose elements were randomly selected from the log-normal permeability distribution. The dimensions of such matrices were determined based on the REVs. To compute the effective permeability in two and three dimensions, permeability was scaled up at the 2×2 block and $2 \times 2 \times 2$ cube levels using Eqs. (4) and (5), respectively. For each geologic formation, we iterated these computations 1000 times and averaged over all to calculate the k_{eff}. The MATLAB code used for the implementation of RGT in both two- and three- dimensions, including a step-by-step explanation, is presented in Appendix B.

To estimate the effective permeability within the EMA framework, we numerically solved Eq. (6) in MATLAB. In two and three dimensions, we set z = 4 and 6, respectively. In Appendix

C, the MATLAB code for implementing the EMA for all formations are presented and explained for both the two- and three- dimensional cases.

3.4. Models evaluation criteria

To evaluate the accuracy of each model, the root mean square log-transformed error (RMSLE) and the relative error (RE) values were calculated as follows

$$RMSLE = \sqrt{\frac{1}{N}\sum_{i=1}^{N}[\log_e(x_{\text{est}}) - \log_e(x_{\text{sim}})]^2} \quad (8)$$

$$RE = \frac{x_{\text{est}} - x_{\text{sim}}}{x_{\text{sim}}} \times 100 \quad (9)$$

where N is the number of samples, and x_{est} and x_{sim} are, respectively, the estimated and simulated values.

Chapter 4 - Results and Discussion

In this chapter, we present the obtained results. The REV plots based on which the representative permeability value for each formation was determined are given in Figures 4-1 and 4-2 for two and three dimensions, respectively. To determine the value of REV and the corresponding permeability, the effective permeability numerically computed via COMSOL was plotted against the domain size for both two- and three-dimensional simulations. Recall that the domain size indicates the number of cells along each side of domain. The representative elementary volume (REV) was accordingly determined for each formation based on these plots.

Comparing Figure 4-1 with Figure 4-2 shows that the REV values in three dimensions are greater than those in two dimensions. The obtained results are consistent with those reported by Marafini et al. (2020). This is because the number of cells within the formation in two dimensions (i.e., $n \times n$ in which n represents the number of cells) is less than that in three dimensions (i.e., $n \times n \times n$) by a factor of the number of cells. This leads the cell arrangement even at random to have a substantial impact on flow simulations.

We also compare the estimated effective permeability values by different models including the ANPT, Eq. (1), SPT, Eq. (2), ALPT, Eq. (3), CPA, RGT, Eq. (4) and (5), and EMA, Eq. (6) with the numerically simulated ones from COMSOL in Figures 4-3 and 4-4 for the 2 and 3D formations, respectively. In Formations 1 through 5, permeability spans about three orders of magnitude ($6.1\times10^{-14} \leq k \leq 3.2\times10^{-11}$), and σ ranges between 0.05 and 0.56. In Formations 6 to 10, however, permeability spans close to eight orders of magnitude ($6.1\times10^{-14} \leq k \leq 3.2\times10^{-5}$), and σ varies between 2 and 6. Formations 1 to 5 represent relatively heterogeneous reservoirs, while Formations 6 to 10 denote heterogeneous systems. In what follows, we address the reliability and accuracy of each model based on its performance in this study.

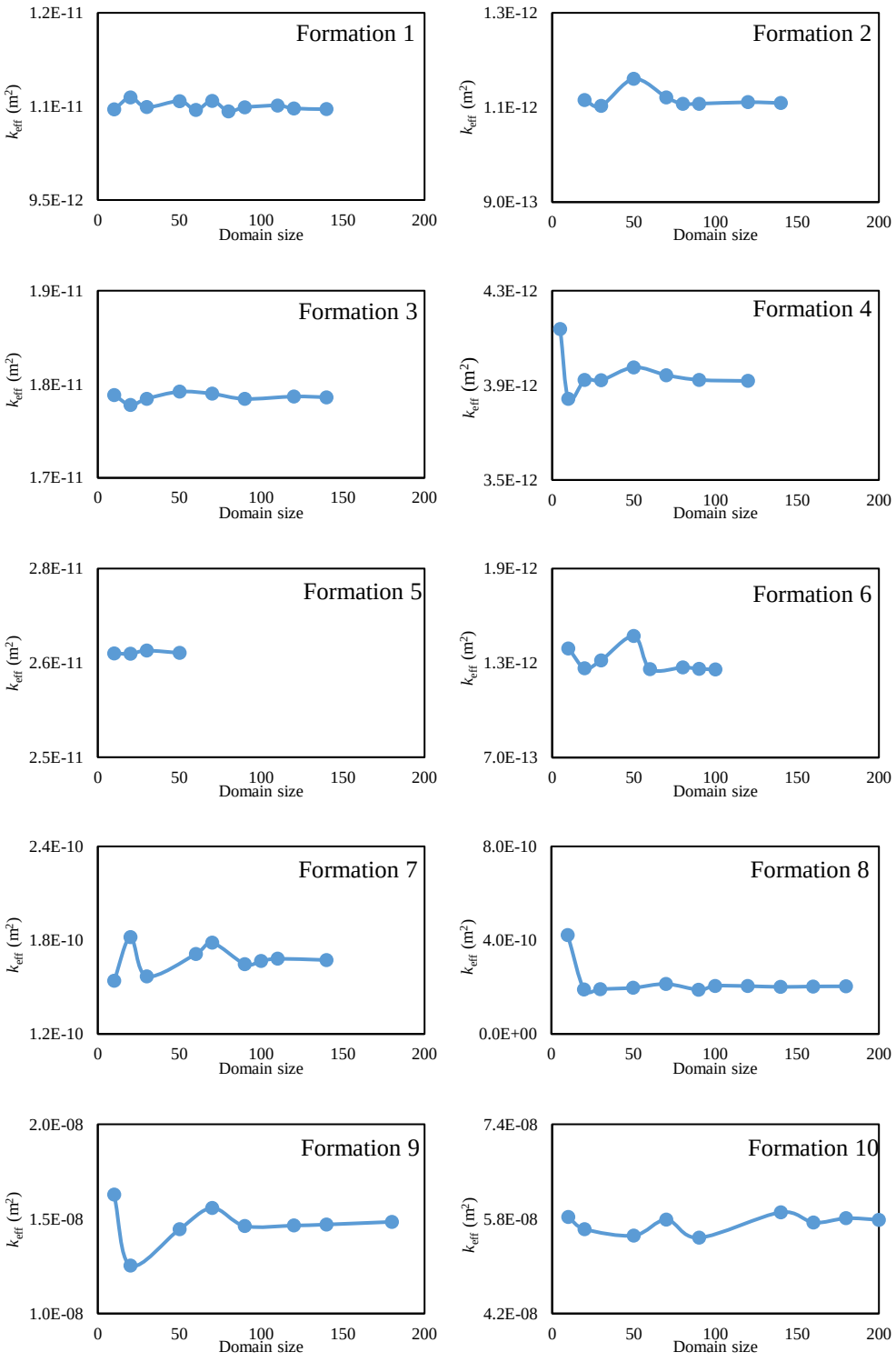

Figure 4-1. Plots of effective permeability against domain size to determine the representative elementary volume (REV) for each of the 2D formations.

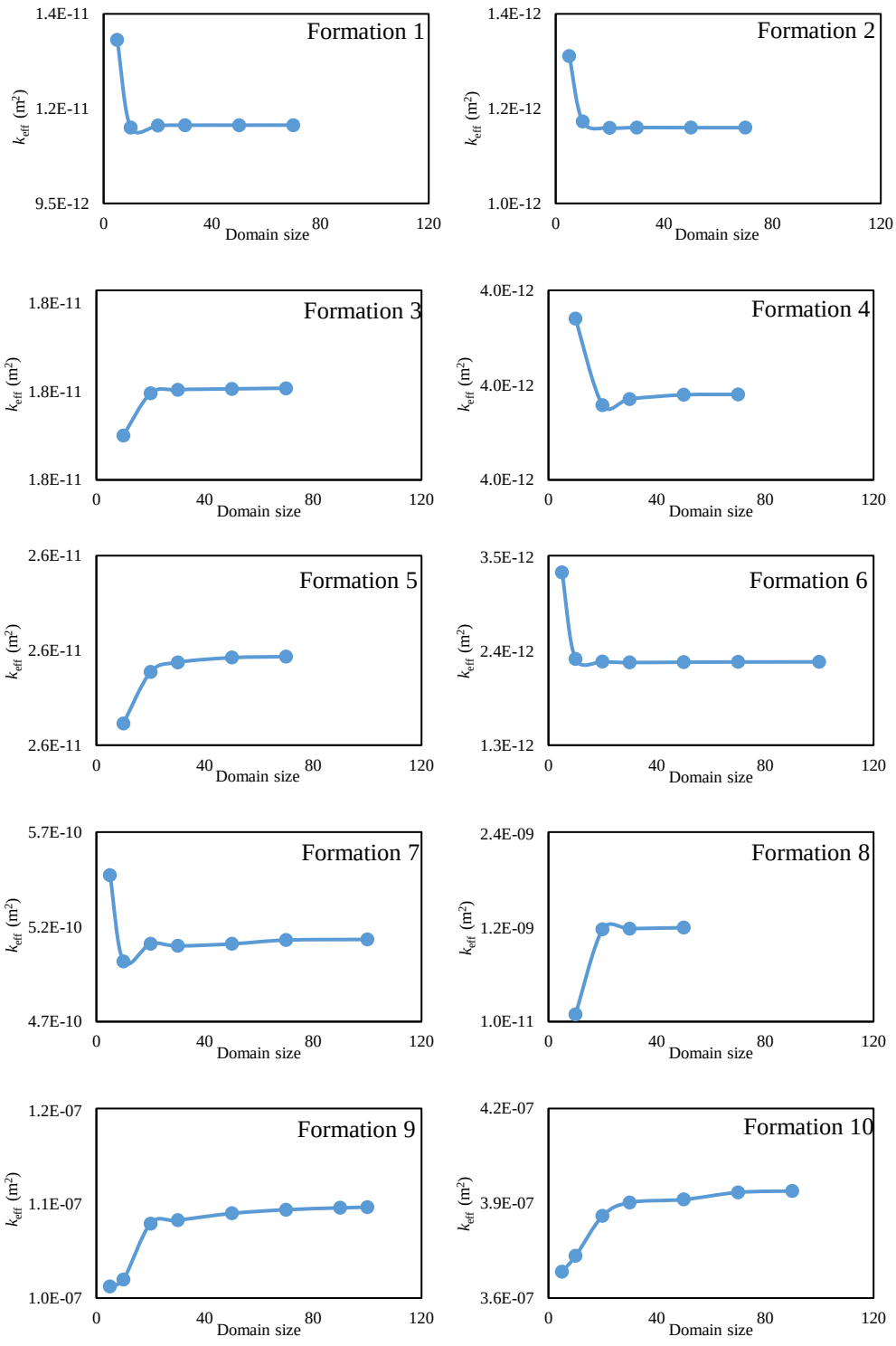

Figure 4-2. Plots of effective permeability against domain size to determine the representative elementary volume (REV) for each of the 3D formations.

4.1. Perturbative methods

In two dimensions, all of the perturbative models i.e., ANPT, SPT, and ALPT estimated the effective permeability accurately in Formations 1 to 5 ($\sigma \leq 0.56$). However, they substantially overestimated the k_{eff} in Formations 6 to 10 ($\sigma \geq 2$) as shown in Figures 4-3a-4-3c. A summary of the RE values calculated for each model estimation is shown in Tables 4.1 and 4.2. We found RMSLE = 15.32, 15.32, and 5.49 respectively for the ANPT, Eq. (1), SPT, Eq. (2), and ALPT, Eq. (3), models. We should note that in two dimensions both the ANPT, Eq. (1), with $\gamma_i = 0$ and $\epsilon = 0$, and SPT, Eq. (2), models reduce to Matheron's conjecture (Matheron, 1967) in which $k_{\text{eff}} = k_{\text{g}}$. As a result, the ANPT and SPT models resulted in the same estimations with RMSLE and average RE values of 15.32 and 1.72×10^{17}% respectively for all the formations. The ALPT returned an average RE value of 1.81×10^{7}% for all formations. Among the three perturbative methods studied here, the ALPT, Eq. (3), provided the most accurate estimations of k_{eff} in two dimensions.

We also investigated the models' accuracy within Formations 1 to 5 and 6 to 10. For the ANPT model we found RMSLE = 0.22 and 21.66, and average RE values of 20% and 3.4×10^{17} % for the k_{eff} estimations, in Formations 1 to 5 and 6 to 10, respectively. The RE values range from 0.14 (Formation 5) to 1.72×10^{18}% (Formation 10). Same results were obtained for the SPT model. For the ALPT model RMSLE values of 0.22 and 7.76 were found with average relative error values of 20% and 3.6×10^{7}% respectively for Formations 1 to 5 and 6 to 10.

Similar results were obtained in three dimensions; the three perturbative methods overestimated the effective permeability in Formations 6 to 10, while they provided accurate estimations in Formations 1 to 5 (Figures 4-4a-4-4c).

Table 4.1 RE (%) of comparisons between k_{eff} estimations and numerical simulation results of k_{eff} for the 2D Formations.

Formation	k_g**(m^2)**	σ	**ANPT**	**SPT**	**ALPT**	**CPA**	**RGT**	**EMA**
1	1.5×10^{-11}	0.56	43.47	43.47	43.40	4.41	-0.81	35.70
2	1.5×10^{-12}	0.56	35.35	35.35	35.30	-1.49	-2.08	34.40
3	1.9×10^{-11}	0.25	8.04	8.04	8.04	1.49	0.1	7.36
4	4.5×10^{-12}	0.40	14.63	14.63	14.60	-2.32	-1.45	14.80
5	2.6×10^{-11}	0.05	0.14	0.14	0.14	-0.11	-0.30	0.02
6	5.0×10^{-11}	2.0	3858	3858	437	-27.50	-12.88	-95.2
7	1.0×10^{-6}	3.0	6.00×10^{5}	6.00×10^{5}	904	-25.97	-49.92	4.96×10^{5}
8	1.0×10^{-3}	4.0	4.93×10^{8}	4.93×10^{8}	6510	-44.51	-63.48	2.23×10^{6}
9	1.0×10^{3}	5.0	6.83×10^{12}	6.83×10^{12}	3.83×10^{12}	-5.20	-71.71	6.80×10^{4}
10	1.0×10^{9}	6.0	1.72×10^{18}	1.72×10^{18}	1.81×10^{8}	299.21	-68.66	2.00×10^{4}

Table 4.2 RE (%) of comparisons between k_{eff} estimations and numerical simulation results of k_{eff} for the 3D Formations.

Formation	k_g**(m^2)**	σ	**ANPT**	**SPT**	**ALPT**	**CPA**	**RGT**	**EMA**
1	1.5×10^{-11}	0.56	41.6	34	41.40	-2.18	4.72	26.30
2	1.5×10^{-12}	0.56	36.2	29	35.90	-5.94	4.54	36.50
3	1.9×10^{-11}	0.25	7.3	6	7.30	-0.24	1.07	58.80
4	4.5×10^{-12}	0.40	14.8	12	14.80	-4.76	2.675	15.00
5	2.6×10^{-11}	0.05	0.37	0.33	0.37	0.08	0.06	0.21
6	5.0×10^{-11}	2.0	2090	2095	57.20	-59.80	36.05	-97.30
7	1.0×10^{-6}	3.0	1.95×10^{5}	1.95×10^{5}	66.50	-75.96	63.54	2.66×10^{5}
8	1.0×10^{-3}	4.0	8.37×10^{7}	8.37×10^{7}	495.00	-90.58	78.17	5.03×10^{5}
9	1.0×10^{3}	5.0	9.13×10^{11}	9.13×10^{11}	2.75×10^{4}	-87.32	80.03	1.03×10^{4}
10	1.0×10^{9}	6.0	2.54×10^{17}	2.54×10^{17}	1.46×10^{7}	-41.05	74.80	3.20×10^{3}

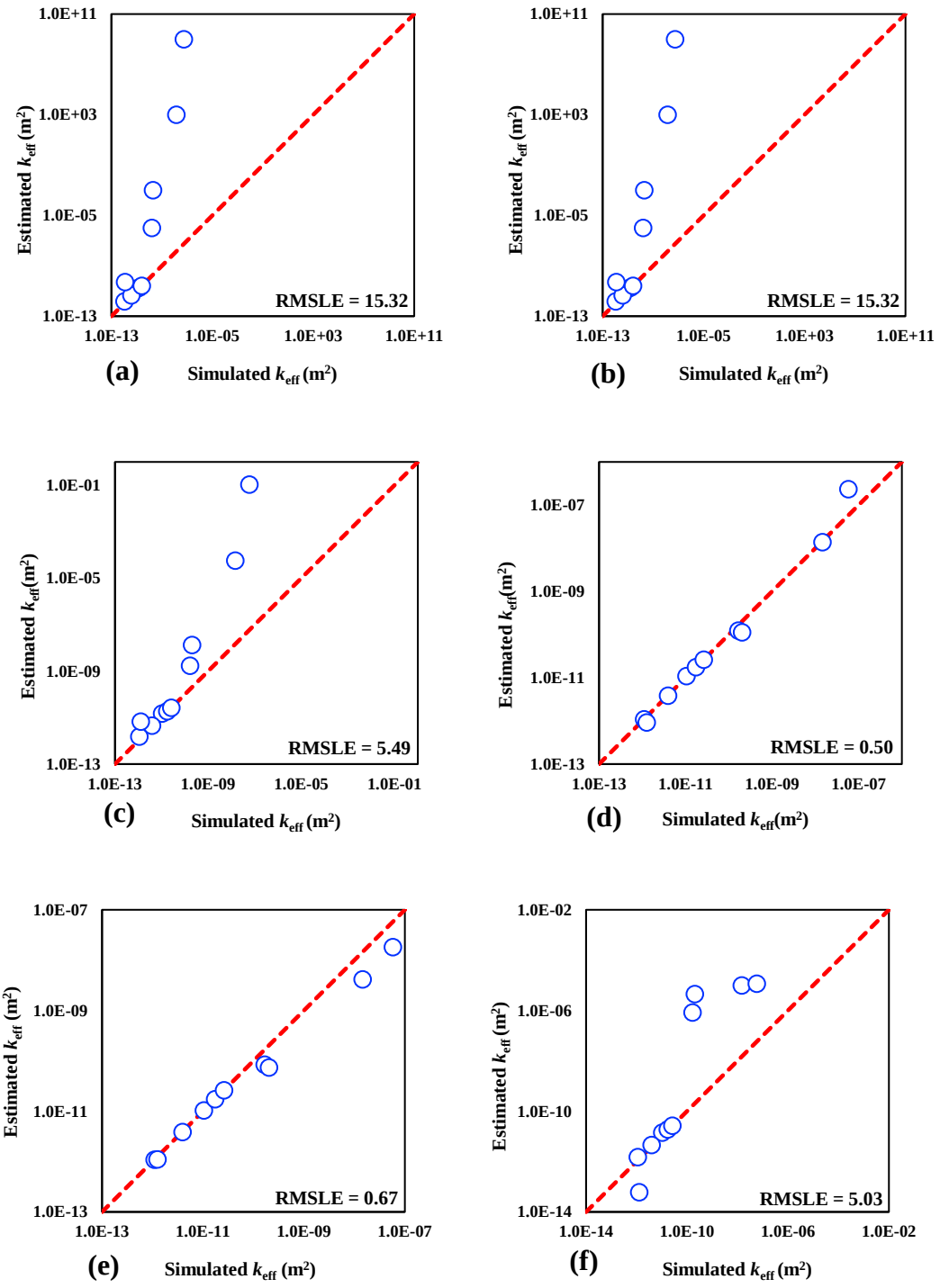

Figure 4-3. Comparison of effective permeabilities calculated from 2D numerical simulations and those estimated from models including (a) ANPT, Eq. (1), (b) SPT, Eq. (2), (c) ALPT, Eq. (3), (d) CPA, (e) RGT, Eq. (4), and (f) EMA, Eq. (6).

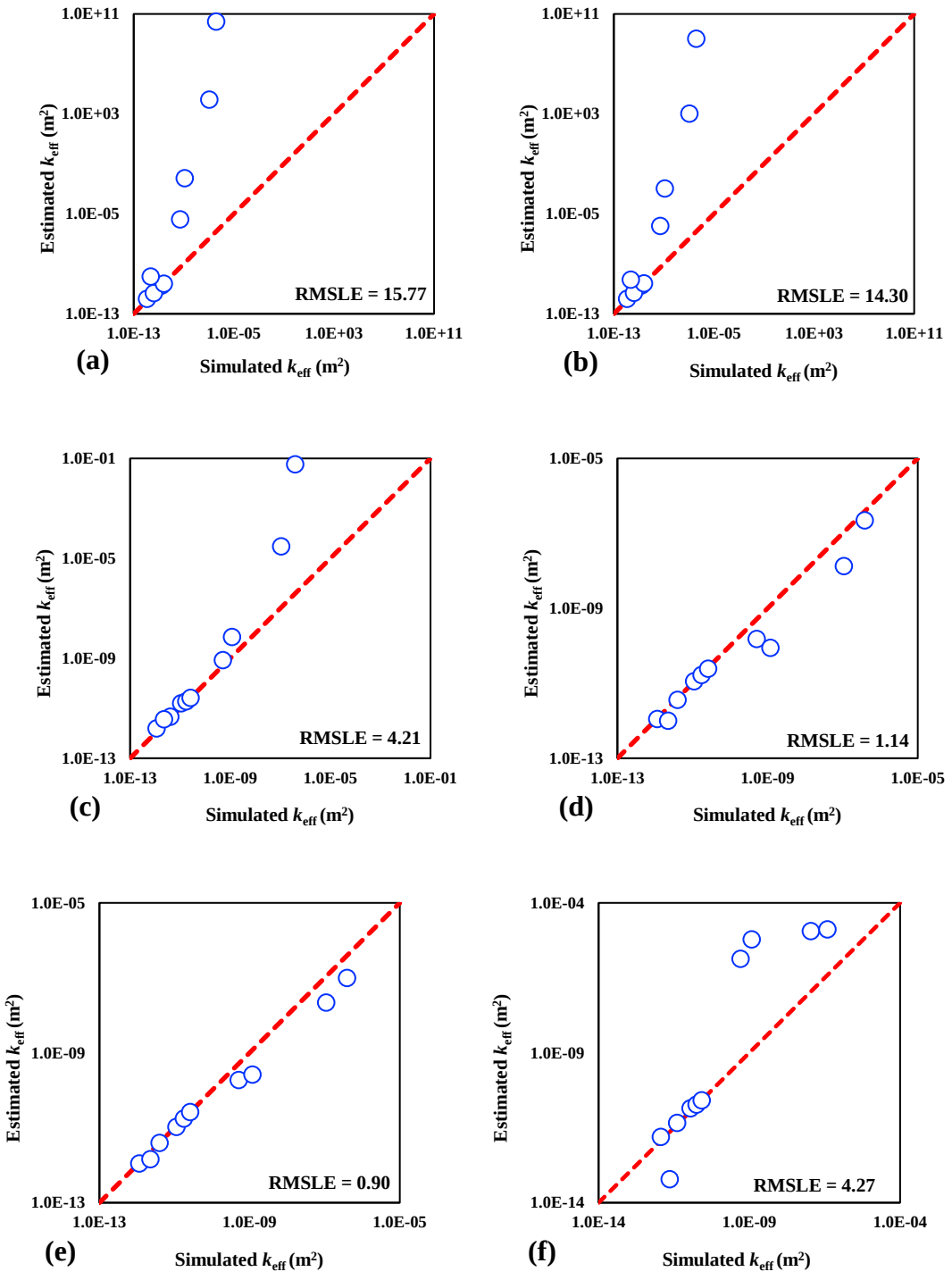

Figure 4-4. Comparison of effective permeabilities calculated from 3D numerical simulations and those estimated from models including (a) ANPT, Eq. (1), (b) SPT, Eq. (2), (c) ALPT, Eq. (3), (d) CPA, (e) RGT, Eq. (4), and (f) EMA, Eq. (6).

We found RMSLE = 15.77, 14.30, and 4.21 and average RE values as $2.54 \times 10^{16}\%$, $2.54 \times 10^{16}\%$, and $1.46 \times 10^{6}\%$ respectively for the ANPT, Eq. (1), SPT, Eq. (2), and ALPT, Eq. (3), models. While the accuracy of the ANPT model estimations in three dimensions reduced compared to the case in two dimensions, the SPT model performed slightly better. The accuracy of the ALPT model also improved from two to three dimensions (RMSLE = 4.21 vs. 5.49).

We also compared the performance of the perturbative methods within Formations 1 to 5 and 6 to 10. Comparison of the estimations by the ANPT with the simulations by COMSOL in Formations 1 to 5 and 6 to 10 showed that this model reasonably estimated k_{eff} in the former (relatively heterogeneous formations) with RMSLE of 0.22, while it overestimated the k_{eff} with RMSLE = 20.18 in the latter (heterogeneous formations). Furthermore, the average RE values of 20% and $5.08 \times 10^{16}\%$ respectively in Formations 1 to 5 and Formations 6 to 10 confirm that the ANPT estimates k_{eff} efficiently in relatively heterogeneous formations but breaks down in very heterogenous formations. Although this model might estimate effective permeability with a higher degree of accuracy in anisotropic formations (Sarris and Paleologos, 2004), it essentially reduces to a form similar to the SPT in case of isotropy. This could be a reason for the substantial overestimations by this model especially for the very heterogeneous formations.

For the SPT model, we found RMSLE values of 0.18 and 20.18 and average RE values of 16% and $5 \times 10^{16}\%$ respectively, similar to those reported in two dimensions. For the ALPT model, however, RMSLE = 0.22 and 5.94, values were less, particularly in Formations 6 to 10, compared to the SPT and ANPT models. The ALPT model underestimated k_{eff} with an average RE of 19.9% in Formations 1 to 5, and overestimated the effective permeability values with an average RE of $2.93 \times 10^{6}\%$, about ten orders of magnitude smaller than that obtained from the SPT in Formations 6 to 10. Our results demonstrate that the ALPT model estimates the effective

permeability accurately in three-dimensional formations with $\sigma \leq 4$. This model performs better than the other perturbative methods probably because of the inverse nature of its formulation, which clearly reduces the amount of overestimations in heterogeneous porous media.

4.2. Critical path analysis

Two-dimensional results from the CPA are presented in Figure 4-3d. As can be seen, the CPA with RMSLE = 0.50 estimated the k_{eff} in all formations accurately (with data points distributed around the 1:1 line indicating well agreement between the numerical simulations and the CPA estimations). We found an average RE value of 19.8% for all formations. Although in most formations the CPA slightly underestimated the effective permeability, it overestimated k_{eff} in Formation 10 with the relative error of 299.21%. Further analysis showed that the CPA estimated k_{eff} with RMSLE = 0.02 and 0.70 within Formations 1 to 5 and 6 to 10, with average RE values of 0.4% and 39.21%, respectively. It is worth pointing out that the average RE for each of the estimations for the relatively heterogeneous formations are all significantly less than 10%, with the highest error of 4.41% in Formation 1.

In three dimensions, CPA also estimated k_{eff} accurately with an RMSLE of 1.14 and average RE of -36.8%. Plots of the estimated effective permeability values against the simulated ones are shown in Figure 4-4d for the three-dimensional formations. We should point out that the CPA estimations are the same in two and three dimensions since the mode of the permeability distribution does not vary with formation dimensionality. Generally speaking, the CPA tended to underestimate the k_{eff} in most 3D formations.

The CPA estimated k_{eff} within Formations 1 to 5 with RMSLE = 0.04 and average relative error of -2.61%. From Formations 6 to 10, the values of RMSLE and average RE were 1.61 and -70.94%, respectively.

4.3. Renormalization group theory

The RGT estimated the effective permeability in 2D formations accurately with RMSLE = 0.67 and average relative error = -27% (Figure 4-3e). It can be deduced from the average RE that the RGT model, Eq. (5), on average, underestimated the k_{eff}. Similar to the CPA, the RGT estimated k_{eff} more accurately in Formations 1 to 5 (RMSLE = 0.012 and average RE = -0.9%) than in Formations 6 to 10 (RMSLE = 0.94 and average RE = -53%).

In three dimensions, the RGT estimated the effective permeability for all ten formations with RMSLE = 0.90 (Figure 4-4e) and average RE = -35% (slightly more accurate than the CPA). Comparison of the estimated k_{eff} values with the simulated values resulted in RMSLE = 0.03 for Formations 1 to 5 and 1.27 for Formations 6 to 10. The average RE values were -3 and -67% in Formations 1 to 5 and 6 to 10, respectively. Similar to the results of CPA, the RGT model tended to underestimate the effective permeability in most formations studied here.

4.4. Effective medium approximation

A plot of the k_{eff} estimations via the EMA against the k_{eff} simulations by COMSOL for the two-dimensional formations is shown in Figure 4-3f. We found RMSLE = 5.03 and average relative error = 2.81×10^{5}%. As can be visually confirmed from the data points lay on the 1:1 line in Figure 4-3f, the EMA accurately estimated the effective permeability in Formations 1 to 5 with RMSLE = 0.20 (similar to the perturbative methods) and average RE = 18%. Although the EMA underestimated k_{eff} in Formation 6 with σ = 2, it overestimated the effective permeability in Formations 7 to 10 ($\sigma \geq 3$). For Formations 6 to 10, however, we found RMSLE = 7.11 and average RE = 5.6×10^{5} %.

Results of the EMA model and its k_{eff} estimations in three dimensions are presented in Figure 4-4f. We found RMSLE = 4.27 and average relative error = 7.8×10^{4}%. Comparing the RMSLE values from two- and three-dimensional results (5.03 vs. 4.27 respectively) shows that

the EMA provided more accurate estimations in three dimensions. Further comparison rendered RMSLE = 0.19 and average RE = 17% in Formations 1 to 5 (similar to the perturbative methods) and RMSLE = 6.03 and average RE = 1.6×10^5%. in Formations 6 to 10. Results (RMSLE and RE values) show that the EMA provides accurate results in relatively heterogenous media (Formations 1 to 5) in both two and three dimensions. However, it mostly overestimates the k_{eff} in formations with $\sigma \geq 2$.

4.5. Models performance

King (1989), Renard and de Marsily (1997), and Sanchez-Vila et al. (2006) amongst others noted that the perturbative methods accurately estimate the effective in media with small variations in permeability but breaks down in heterogeneous ones. Similar results were obtained by Dykaar and Kitanidis (1992), Neuman et al. (1992) and Hristopulos and Christakos (1999) who showed that Matheron's conjecture and many of the perturbative methods can be successfully applied to permeability distributions with σ values up to 2.65. Similarly, evidence from this study showed substantial effective permeability overestimations by several perturbative methods in the statistically heterogeneous permeability distributions ($\sigma \geq 2$).

Most perturbative methods reduce to the exact form of the conjecture (k_{eff}=k_{g}) in two-dimensions. Although the ANPT and SPT models include terms in their expressions other than the permeability variance, these models essentially reduce to Matheron's conjecture when applied to two-dimensional isotropic geologic formations. Therefore, it is not surprising that the perturbative methods used in this study substantially overestimated the effective permeability in the statistically heterogeneous geologic formations ($\sigma \geq 2$). However, the ALPT does not reduce to the exact form of the conjecture and this, in addition to the inverse form of its k_{eff} expression, could account for the higher accuracy of this model.

Applying the conjecture to 3D formations did not result in accurate estimations of k_{eff} (results not shown), as expected. While the k_{eff} estimations by the SPT model improved from 2D to 3D (see RMSLE values), the ANPT model deteriorated in 3D. Also, the inclusion of the k_{eff} dependence on the permeability distribution function in the ANPT, SPT, and ALPT models made no positive impact on the effective permeability estimations in the heterogeneous formations (large σ). Except in few cases, the perturbative methods resulted in substantial overestimations of the effective permeability in the statistically heterogeneous geologic formations. Among the perturbative methods studied here, the ALPT provided the best estimations in 2 and 3D. This model performs almost as accurate as the EMA; see the reported RMSLE values in Figures 4-3 and 4-4 as well as the relative errors in Table 4.1.

CPA has been successfully applied to estimate the k_{eff} at the core scale (Katz and Thompson, 1986; Ghanbarian et al., 2016; 2017; Ghanbarian, 2020;). However, its applications at the field scale are very limited. Hunt and Idriss (2009) applied concepts from CPA to determine the effective permeability in correlated and random systems with bimodal permeability distributions in terms of the arithmetic mean of $k_{min} < k < k_{max}$ and harmonic mean of $k_c < k < k_{max}$ in which k_c is the critical permeability. They showed that the CPA provided reasonable estimations above the percolation threshold in correlated systems. From our findings, the CPA estimated the effective permeability of the geologic formations in two and three dimensions with a high degree of accuracy. Although for the log-normal permeability distribution the value of k_{eff} is determined from k_{g} and σ, our proposed CPA approach is quite general and applicable to any unimodal distribution, which makes its application general and independent of the shape of the permeability distribution. In addition, CPA estimations are

dimension independent, in contrast to the perturbative methods and the other models applied in this study.

While CPA estimated the k_{eff} with the highest degree of accuracy compared to all other methods in the 2D geologic formations (as seen from RMSLE values), it estimated k_{eff} with an RMSLE value smaller than all but the RGT in three dimensions. We found that the CPA underestimated the k_{eff} in the geologic formations with average RE that are orders of magnitude smaller than those produced by most of the other models applied in this study. This is in stark contrast to the results derived from the perturbative methods, which generally tended to overestimate k_{eff} with high error values, especially in the statistically heterogeneous formations. A possible reason for the success of this technique could be its inherent dependence on the flow paths of the porous medium rather than the statistical parameters that describe the permeability distribution.

Several studies in the literature have highlighted the success of the RGT in estimating the effective permeability of homogenous and heterogeneous formations including King (1989); Hristopulos and Christakos (1999); Green and Paterson (2007); Sadeghnejad and Masihi (2017) and many others. Hristopulus and Christakos (1999) applied concepts from RGT and surprisingly provided k_{eff} estimations that were closer to experimental results than numerical simulation results by a factor of eight.

King (1989) also showed good agreement between k_{eff} estimations by RGT and numerically simulated k_{eff} in synthetic and real datasets. In his work, which was performed on uniformly and log-normally distributed permeability fields, he found that the RGT estimated k_{eff} within 1% of direct simulation result. He also pointed out that perturbative methods and geometric mean did

not provide reliable estimations of k_{eff} at large variance values but the agreement of renormalization with simulation results within 3% for the large variances.

In the same way, RGT estimated k_{eff} with a high degree of accuracy for all two- and three-dimensional formations in this work. Among all the models applied in this work, the RGT estimated k_{eff} with the highest degree of accuracy in the 3D geologic formations. Similar to CPA, the RGT also mostly underestimated the effective permeability of the geologic formations as seen from the RE values. Although fluid flow in heterogeneous porous media is neither perfectly in series nor parallel as assumed in the 3D RGT, the analogy of this method to the flow of current in electrical resistors seem to result in accurate estimations.

The EMA model is not based on perturbation theory expansions, but is derived by setting an average perturbation of a heterogeneous system equal to zero, and this could be a reason why it mostly overestimated k_{eff}. However, the model estimated k_{eff} with a high level of accuracy, particularly in Formations 1 to 5 (based on RMSLE values).

It is well documented in the literature that the EMA returns accurate estimations for permeability distributions with small variance values (Adler and Berkowitz, 2000; Ghanbarian and Daigle, 2016). For example, Adler and Berkowitz (2000) evaluated the accuracy of electrical conductivity estimations by EMA in two- and three-dimensional media with local conductances that followed the lognormal distribution with various standard deviations. They concluded that, "... the analytical expressions [the effective-medium approximations] provide good agreement to the simulations in 2D systems, but are in significant error in 3D systems when the standard deviation of the local conductivities is large."

Ghanbarian and Daigle (2016) also showed that the EMA overestimated the k_{eff} significantly when $\log(k_{\max}/k_{\min}) > 0.8$. For the relatively heterogenous formations (Formations 1 to 5) in

this study, $\log(k_{\max}/k_{\min})$ = 2.7, while the value is equal to 8.6 in the heterogeneous formations (Formations 6 to 10). Therefore, the EMA performed robustly in estimating the k_{eff} values in Formations 1 to 5.

In summary, the CPA and RGT models estimated the effective permeability in relatively heterogeneous (Formations 1 to 5) and heterogeneous (Formations 6 to 10) reservoirs with the smallest RMSLE values. Although the RGT estimated k_{eff} for all the geologic formations more accurately in three dimensions (based on RMSLE values) than any other model in this work, the CPA estimations were closest to numerical simulation results in two dimensions. However, it should be noted that RGT is a recursive algorithm (Renard and de Marsily, 1997) that is determined by a series of successive aggregations. In contrast, CPA requires no calculation, computation, nor computer programming, etc. In fact, CPA saves a substantial demand in computations and time with precise estimations in two and three dimensions.

4.6. 2D versus 3D simulations

Results showed that the k_{eff} values from two- and three-dimensional simulations were highly correlated. More specifically, we found $\left(k_{eff}\right)_{3D} = 234.14\left(k_{eff}\right)_{2D}^{1.2}$ with R^2 = 0.99. In all formations except Formation 5 the value of k_{eff} in three dimensions was greater than that in two dimensions (Table 1). This is consistent with the results of King (1989) and Adler and Berkowitz (2000). More specifically, King (1989) simulated the k_{eff} in two- and three-dimensional systems with uniform and log-normal permeability distributions and reported k_{eff} in three dimensions greater than that in two dimensions.

4.7. Long-range correlation and anisotropy

It is well documented in the literature that there might exist long-range correlation at the aquifer/reservoir scale (Clark et al., 2020; Sahimi, 2011; Sahimi and Mukhopadhyay, 1996).

Correlation means that heterogeneity e.g., permeability in one zone of a geologic formation is not fully independent of that in other zones. Correlation often presents at all length scales. Sahimi (1994) stated that natural porous media are not necessarily random and may exhibit some correlation. For instance, core-scale porous media may contain only short-range correlations, while heterogeneous field-scale formations, such as aquifers and reservoirs, may be long-range correlated.

Geologic formations might also be anisotropic at such scales. In general, there might be three types of anisotropy in geological structures: (I) A formation may consist of randomly oriented anisotropic permeability blocks, (II) the distribution of permeability may be direction-dependent, and (III) anisotropy due to the presence of permeability zones of different orientations with different probabilities of being available to flow (Mukhopadhyay and Sahimi, 2000). In type I, the effective permeability of such formations is always isotropic. In type II, the anisotropy may vanish under certain circumstances, while in type III anisotropy always remains (Mukhopadhyay and Sahimi, 2000).

In this study, we evaluated the CPA approach in isotropic and uncorrelated (random) formations. Further investigations are required to assess the reliability and predictability of the CPA in anisotropic and correlated large-scale porous media.

Chapter 5 - Conclusions

Using concepts from critical path analysis (CPA), we presented a novel, simple, and robust approach to estimate the effective permeability at the reservoir scale. Based on the CPA, lower permeability zones in a geologic formation contribute little or nothing to the overall permeability, while higher permeability zones provide the paths through which fluid flows. We postulated that permeability at the mode of permeability density function should represent the effective permeability of a reservoir. The reliability of the proposed CPA approach was evaluated by comparing with two- and three-dimensional simulations in ten geologic formations with different levels of heterogeneity. The truncated log-normal permeability distribution with different geometric means ($4.5\times10^{-12}\leq k_g \leq1.0\times10^{9}$ m^2) and standard deviations ($0.05\leq \sigma \leq6$) was used to generate such formations. In addition to the CPA, other theoretic approaches, such as perturbation theory-based methods, effective medium approximation, and renormalization group theory, were applied to estimate the k_{eff}. Results showed that the CPA estimated the k_{eff} with RMSLE = 0.50 more accurate than the other approaches in two dimensions. However, renormalization group theory with RMSLE = 0.90 estimated the k_{eff} slightly more accurate than the CPA with RMSLE = 1.14 in three dimensions. We also found that both perturbation theory and the effective-medium approximation provided reasonable estimations of k_{eff} in formations with permeability standard deviation $\sigma < 2$. However, these two approaches substantially overestimated the effective permeability in highly heterogeneous formations with $\sigma > 2$. Further investigations are required to evaluate the reliability of the CPA approach in correlated and anisotropic geologic formations.

References

Adler, P.M., Berkowitz, B., 2000. Effective medium analysis of random lattices. Transp. Porous Media 40, 145–151. https://doi.org/10.1023/A:1006611011600

Akpoji, G.A., De Smedt, F., 1993. Assessment of the effective hydraulic conductivity with a numerical model. Trans. Ecol. Environ. 2, 101–108.

Ambegaokar, V., Halperin, B.I., Langer, J.S., 1971. Hopping conductivity in disordered systems. Phys. Rev. B 4, 2612–2620.

Attinger, S., Eberhard, J., Neuss, N., 2002. Computing and Visualization in Science Filtering procedures for flow in heterogeneous porous media : numerical results. Water Resour. Manag. 72, 67–72.

Bjerg, P.L., Hinsby, K., Christensen, T.H., Gravesen, P., 1992. Spatial variability of hydraulic conductivity of an unconfined sandy aquifer determined by a mini slug test. J. Hydrol. 136, 107–122.

Clark, C.L., Winter, C.L., Corley, T., 2020. Effects of percolation on the effective conductivity of irregular composite porous media. Adv. Water Resour. 137, 103507.

Colecchio, I., Boschan, A., Otero, A.D., Noetinger, B., 2020. On the multiscale characterization of effective hydraulic conductivity in random heterogeneous media: a historical survey and some new perspectives. Adv. Water Resour. 140, 103594.

Dagan, G., 1993. Higher-order correction of effective permeability of heterogeneous isotropic formations of lognormal conductivity distribution. Transp. Porous Media 12, 279–290.

Dagan, G., 1989. Flow and Transport in Porous Formations. Springer 465.

Dagan, G., 1979. Models of groundwater flow in statitically homogeneous porous formations. Water Resour. Res. 15, 47–63.

Dagan, G., Fiori, A., Jankovic, I., 2013. Upscaling of flow in heterogeneous porous formations : Critical examination and issues of principle. Adv. Water Resour. 51, 67–85. https://doi.org/10.1016/j.advwatres.2011.12.017

De Wit, A., 1995. Correlation structure dependence of the effective permeability of heterogeneous porous media. Phys. Fluids 7, 2553–2562. https://doi.org/10.1063/1.868705

Deutsch, C., 1989. Calculating effective absolute permeability in sandstone/shale sequences. SPE Form. Eval. 4, 343–348.

Dykaar, BB., K.P., 1992. Determination of the effective hydraulic conductivity 2., for heterogeneous porous media using a numerical spectral approach. Water Resour Res 28, 1167–1178.

Edery, Y., Guadagnini, A., Scher, H., Berkowitz, B., 2014. Origins of anomalous transport in heterogeneous media: Structural and dynamic controls. Water Resour. Res. 50, 1490–1505.

Fogg, G.E., 2010. Log-K variance, connectivity, unconformities and non-Fickian transport, in: Geol. Soc. Am. Abstr. Programs. p. 42.

Fokker, P.A., 2001. General anisotropic effective medium theory for the effective permeability of heterogeneous reservoirs. Transp. Porous Media 44, 205–218. https://doi.org/10.1023/A:1010770623874

Freeze, R.A., Cherry,J.A., 1979. Groundwater. New Jersey.

Gelhar, L.W., Axness, C.L., 1983. Three-dimensional stochastic analysis of macrodispersion in aquifers. Water Resour. Res. 19, 161–180. https://doi.org/10.1029/WR019i001p00161

Ghanbarian, B., 2020. Applications of critical path analysis to uniform grain packings with narrow conductance distributions: I. Single-phase permeability. Adv. Water Resour. 137, 103529.

Ghanbarian, B., Hunt, A.G., Skaggs, T.H., Jarvis, N., 2017. Upscaling soil saturated hydraulic conductivity from pore throat characteristics. Adv. Water Resour. 104, 105–113. https://doi.org/10.1016/j.advwatres.2017.03.016

Ghanbarian, B., Daigle, H., 2016. Permeability in two-component porous media: Effective-medium approximation compared with lattice-Boltzmann simulations. Vadose Zo. J. 15. https://doi.org/10.2136/vzj2015.05.0071

Ghanbarian, B., Torres-Verdín, C., Skaggs, T.H., 2016. Quantifying tight-gas sandstone permeability via critical path analysis. Adv. Water Resour. 92, 316–322. https://doi.org/10.1016/j.advwatres.2016.04.015

Green, C. P., Paterson, L., 2007. Analytical three-dimensional renormalization for calculating effective permeabilities. Transp. Porous Media 68, 237–248. https://doi.org/10.1007/s11242-006-9042-y

Gutjahr, A. L., Gelhar, L. W., Bakr, A. A., and MacMillan, J.R., 1978. Stochastic analysis of spatial variability in subsurface flows: 2. Eval. Appl. Water Resour 14, 953–959.

Haneberg, W., 2012. Computational geosciences with Mathematica. Springer Science & Business Media.

Hristopulos, D.T., 2003. Renormalization group methods in subsurface hydrology: Overview and applications in hydraulic conductivity upscaling. Adv. Water Resour. 26, 1279–1308. https://doi.org/10.1016/S0309-1708(03)00103-9

Hristopulos, D.T., Christakos, G., 1999. Renormalization group analysis of permeability upscaling. Stoch. Environ. Res. Risk Assess. 13, 131–160. https://doi.org/10.1007/s004770050036

Hunt, A., Ewing, R., Ghanbarian, B., 2014. Percolation theory for flow in porous media.

Hunt, A.G., 2001. Applications of percolation theory to porous media with distributed local conductances. Adv. Water Resour. 24, 279–307. https://doi.org/10.1016/S0309-1708(00)00058-0

Hunt, A.G., Idriss, B., 2009. Percolation-based effective conductivity calculations for bimodal distributions of local conductances. Philos. Mag. 89, 1989–2007. https://doi.org/10.1080/14786430802660431

Indelman, P., and Abramovich, B., 1994. A higher-order approximation to effective conductivity in media of anisotropic random structure. Water Resour. Res. 30, 1857–1864.

Jankovic, I., Fiori, A., Dagan, G., 2003. Effective conductivity of an isotropic heterogeneous medium of lognormal conductivity distribution. Multiscale Model. Simul. 1, 40–56. https://doi.org/10.1137/S1540345902409633

Janković, I., Fiori, A., Dagan, G., 2003. Flow and transport in highly heterogeneous formations: 3. Numerical simulations and comparison with theoretical results. Water Resour. Res. 39, 1–13. https://doi.org/10.1029/2002WR001721

Katz, A. J., Thompson, A.H., 1986. Quantitative prediction of permeability in porous rock. Phys. Rev. B 34, 8179–8181.

King, P.R., 1989. The use of renormalization for calculating effective permeability. Transp. Porous Media 4, 37–58. https://doi.org/10.1007/BF00134741

Kirkpatrick, S., 1973. Percolation and conduction. Rev. Mod. Phys. 45, 574– 588. https://doi.org/10.1103/RevModPhys.45.574

Marafini, E., La Rocca, M., Fiori, A., Battiato, I., Prestininzi, P., 2020. Suitability of 2D modelling to evaluate flow properties in 3D porous media. Transp. Porous Media 134, 315–329.

Masihi, M., Gago, P.A., King, P.R., 2016. Estimation of the Effective Permeability of Heterogeneous Porous Media by Using Percolation Concepts. Transp. Porous Media 114, 169–199. https://doi.org/10.1007/s11242-016-0732-9

Matheron, G. (1967), 1967. Elements pour une Theorie des Milieux Poruex. Masson.

Mukhopadhyay, S., Sahimi, M., 2000. Calculation of the effective permeabilities of field-scale porous media. Chem. Eng. Sci. 55, 4495–4513. https://doi.org/10.1016/S0009-2509(00)00098-1

Neuman, S. P., Orr, S., Levin, O., & Paleologos, E., 1992. Theory and high-resolution finite element analysis of 2-D and 3-D effective permeabilities in strongly heterogeneous porous media., in: Proceedings of the 9th International Conference on Computational Methods in Water Resources.

Oladele, S., Salami, R., Adeyemi, B.O., 2019. Petrophysical and Rock Physics Analyses for Characterization of Complex Sands in Deepwater Niger Delta, Nigeria. Geosci. Eng. 65, 24–35. https://doi.org/10.35180/gse-2019-0009

Pike, R., Stanley, H.E., 1981. Order propagation near the percolation threshold. J. Phys. A. Math.

Pollak, M., 1972. A percolation treatment of dc hopping conduction. J. Non. Cryst. Solids 11, 1–24.

Rasaei, M.R., Sahimi, M., 2009. Upscaling of the permeability by multiscale wavelet transformations and simulation of multiphase flows in heterogeneous porous media. Comput. Geosci. 13, 187–214. https://doi.org/10.1007/s10596-008-9111-0

Rehfeld, K.R., Boggs, K.M., Gelhar, L.W., 1992. Field Study of Dispersion in a Heterogeneous Aquifer, 3. Geostatistical Analysis of Hydraulic Conductivity. Water Resour. Res. 28, 16.

Renard, P., de Marsily, G., 1997. Calculating equivalent permeability: a review. Adv. Water

Resour. 20, 253–278. https://doi.org/10.1016/S0309-1708(96)00050-4

Reynolds, P.J., Stanley, H.E., Klein, W., 1977. A real-space renormalization group for site and bond percolation. J. Phys. C Solid State Phys. 10, 167–172. https://doi.org/10.1088/0022-3719/10/8/002

Sadeghnejad, S., Masihi, M., 2017. Analysis of a more realistic well representation during secondary recovery in 3-D continuum models. Comput. Geosci. 21, 1035–1048. https://doi.org/10.1007/s10596-017-9640-5

Sahimi, M., 2011. Flow and transport in porous media and fractured rock: From classical methods to modern approaches, 2nd ed. Wiley-VCH, Weinheim, Germany.

Sahimi, M., 1994. Long-range correlated percolation and flow and transport in heterogeneous porous media. J. Phys. I 4, 1263–1268.

Sahimi, M., Mukhopadhyay, S., 1996. Scaling properties of a percolation model with long-range correlations. Phys. Rev. E. Stat. Phys. Plasmas. Fluids. Relat. Interdiscip. Topics 54, 3870–3880. https://doi.org/10.1103/PhysRevE.54.3870

Sanchez-Vila, X., Guadagnini, A., Carrera, J., 2006. Representative hydraulic conductivities in saturated grqundwater flow. Rev. Geophys. 44, 1–46. https://doi.org/10.1029/2005RG000169

Sarris, T.S., Paleologos, E.K., 2004. Numerical investigation of the anisotropic hydraulic conductivity behavior in heterogeneous porous media. Stoch. Environ. Res. Risk Assess. 18, 188–197. https://doi.org/10.1007/s00477-003-0171-3

Stepanyants, Y.A., Teodorovich, E. V., 2003. Effective hydraulic conductivity of a randomly heterogeneous porous medium. Water Resour. Res. 39. https://doi.org/10.1029/2001WR000366

Stinchcombe, R.B., Watson, B.P., 1976. Renormalization group approach for percolation conductivity. J. Phys. C Solid State Phys. 9, 3221–3247. https://doi.org/10.1088/0022-3719/9/17/017

Sudicky, E.A., 1986. A natural gradient experiment on solute transport in a sand aquifer: Spatial variability of hydraulic conductivity and its role in the dispersion process. Water Resour. Res. 22, 2069–2082.

Wainwright, J., Mulligan, M., 2013. Environmental modelling: finding simplicity in complexity. John Wiley & Sons.

Wood, B.D., Taghizadeh, E., 2020. A primer on information processing in upscaling. Adv. Water Resour. 146. https://doi.org/10.1016/j.advwatres.2020.103760

Zarlenga, A., Janković, I., Fiori, A., Dagan, G., 2018. Effective Hydraulic Conductivity of Three-Dimensional Heterogeneous Formations of Lognormal Permeability Distribution: The Impact of Connectivity. Water Resour. Res. 54, 2480–2486.

Appendix A

Formation 1

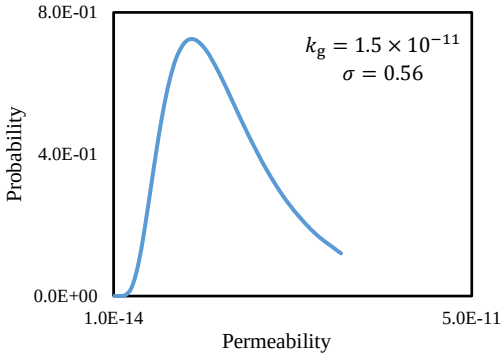

Formation 2

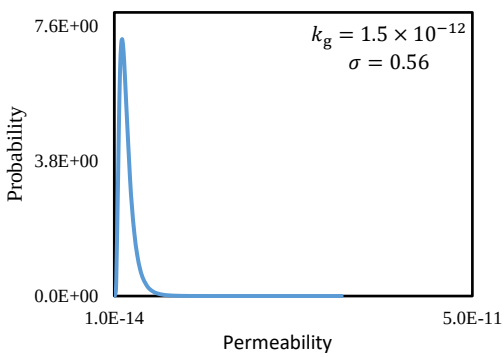

Formation 3

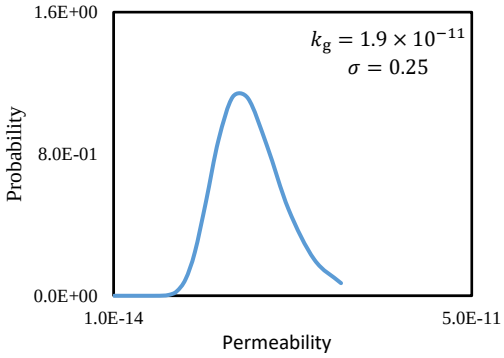

Formation 4

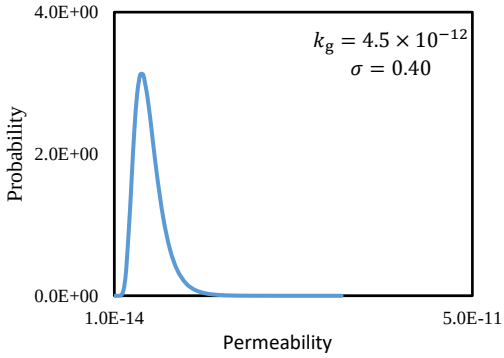

Formation 5

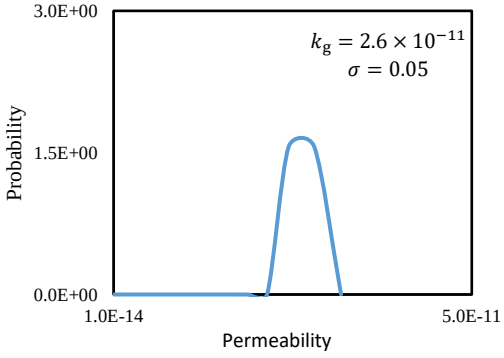

Formation 6

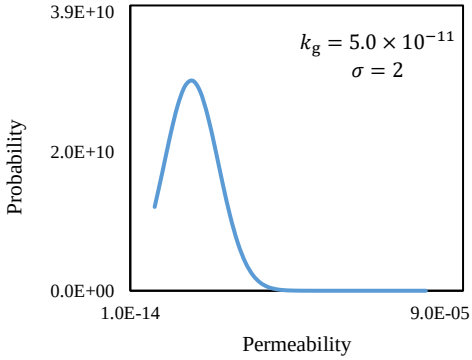

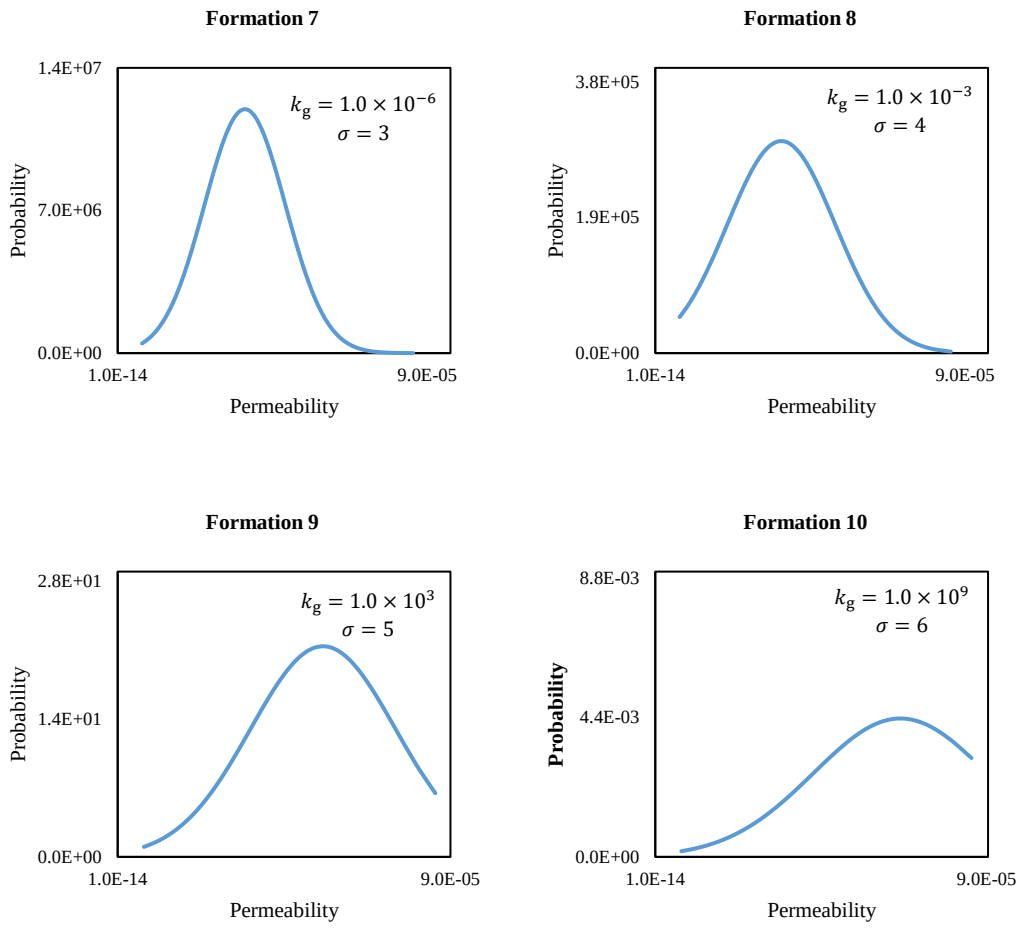

Figure A-1: Permeability probability density function (pdf) for Formations 1-10

Appendix B

The MATLAB code developed to estimate the effective permeability using Renormalization Group Theory (RGT) in ten formations studied here.

RGT in two-dimensional formations

```
% This code estimates the effective permeability of a 2D permeability distribution based on RGT


clear all
clc


% The number of times the code will be iterated
numm=1000;
result=zeros(numm,1);


% Using a for loop for the iteration
for count=1:numm
% nnn=number of steps
nnn=8;
LL=6^nnn;   %total number of boxes


r=sqrt(LL);         % r indicates rows in the permeability matrix for RGT
c=sqrt(LL);         % r indicates columns in the permeability matrix for RGT
N=r*c;
```

% Writing a function to define the RGT expressions for estimating effective permeability of a 2D formation

```
funn=@(x1,x2,x3,x4)
4*(x1+x3)*(x2+x4)*(x2*x4*(x1+x3)+x1*x3*(x2+x4))/((x2*x4*(x1+x3)+(x1*x3)*(x2+x4))*(x1
+x2+x3+x4)+3*(x1+x2)*(x3+x4)*(x1+x3)*(x2+x4));
```

% importing the input permeability data for RGT

```
k1=import permeabilitydata.txt
```

% Reshaping the permeability into a row matrix of N elements

```
Perm1=reshape(permeabilitydata,[N,1]);
```

% Randomizing the permeability values

```
Perm2=Perm1(randperm(numel(Perm1)));
```

% reshaping the random Perm2 row matrix into a matrix with size [r,c]

```
k_renorm=reshape(Perm2,[r,c]);
```

% initializing the size of the k_renorm matrix

```
[nx,ny]=size(k_renorm);
```

```
% defining the new permeability matrix derived from first step of renormalization
k2=zeros(64,64);
% using a for loop to invoke the RGT expression in the first step of renormalization
for i=1:2:c-1
   for j=1:2:r-1
      k2(i,j)=funn(k1(i,j),k1(i,j+1),k1(i+1,j), k1(i+1,j+1));
   end
end
% Removing all elements of the matrix equal to zero
k2=nonzeros(k2');
% Reshaping the final matrix derived from renormalization first step
k2=reshape(k2,64,64)';

% defining the new permeability matrix derived from first step of renormalization
k3=zeros(32,32);
% using a for loop to invoke the RGT expression in the second step of renormalization
for i=1:2:c/2-1
   for j=1:2:r/2-1
      k3(i,j)=funn(k2(i,j),k2(i,j+1),k2(i+1,j), k2(i+1,j+1));
   end
end
% Removing all elements of the matrix equal to zero
k3=nonzeros(k3');
```

```
% Reshaping the final matrix derived from renormalization second step
k3=reshape(k3,32,32)';

% defining the new permeability matrix derived from second step of renormalization
k4=zeros(16,16);
% using a for loop to invoke the RGT expression in the third step of renormalization
for i=1:2:c/4-1
   for j=1:2:r/4-1
      k4(i,j)=funn(k3(i,j),k3(i,j+1),k3(i+1,j), k3(i+1,j+1));
   end
end
% Removing all elements of the matrix equal to zero
k4=nonzeros(k4');
% Reshaping the final matrix derived from renormalization third step
k4=reshape(k4,16,16)';

% defining the new permeability matrix derived from third step of renormalization
k5=zeros(8,8);
% using a for loop to invoke the RGT expression in the fourth step of renormalization
for i=1:2:c/8-1
   for j=1:2:r/8-1
      k5(i,j)=funn(k4(i,j),k4(i,j+1),k4(i+1,j), k4(i+1,j+1));
   end
```

```
end
% Removing all elements of the matrix equal to zero
k5=nonzeros(k5');
% Reshaping the final matrix derived from renormalization fourth step
k5=reshape(k5,8,8)';

% defining the new permeability matrix derived from fourth step of renormalization
k6=zeros(4,4);
% using a for loop to invoke the RGT expression in the fifth step of renormalization
for i=1:2:c/16-1
   for j=1:2:r/16-1
      k6(i,j)=funn(k5(i,j),k5(i,j+1),k5(i+1,j), k5(i+1,j+1));
   end
end
% Removing all elements of the matrix equal to zero
k6=nonzeros(k6');
% Reshaping the final matrix derived from renormalization fifth step
k6=reshape(k6,4,4)';

% defining the new permeability matrix derived from fifth step of renormalization
k7=zeros(2,2);
% using a for loop to invoke the RGT expression in the sixth step of renormalization
for i=1:2:c/32-1
```

```
    for j=1:2:r/32-1
        k7(i,j)=funn(k6(i,j),k6(i,j+1),k6(i+1,j), k6(i+1,j+1));
    end

end
% Removing all elements of the matrix equal to zero
k7=nonzeros(k7');
% Reshaping the final matrix derived from renormalization sixth step
k7=reshape(k7,2,2)';

% defining the new permeability matrix derived from sixth step of renormalization
k8=zeros(1,1);
% using a for loop to invoke the RGT expression in the seventh step of renormalization
for i=1:2:c/64-1
    for j=1:2:r/64-1
        k8(i,j)=funn(k7(i,j),k7(i,j+1),k7(i+1,j), k7(i+1,j+1));
    end

end
% Removing all elements of the matrix equal to zero
k8=nonzeros(k8');

% Writing the effective permeability derived from RGT for each iteration
```

```
result(count)=k8;
end

% Exporting the 1000 effective permeability values into an excel file
RenormPerm=[result];
xlswrite('RenormPerm.xlsx', RenormPerm)
```

RGT in three-dimensional formations

```
% This code estimates the effective permeability of a 3D permeability distribution based on RGT
clear all
clc

% The number of times the code will be iterated
numm=1000;
result=zeros(numm,1);
% Using a for loop for the iteration
for count=1:numm
% nnn=number of steps
nnn=8;
LL=8^nnn;   %total number of boxes

r=(LL).^(1/3);          % r indicates rows in the permeability matrix
c=(LL).^(1/3);          % c indicates columns in the permeability matrix
```

```
N=r*c*r;                    % total number of permeability elements for 3D renormalization

% Writing a function to define the RGT expressions for estimating effective permeability of a 3D
formation
funn=@(x1,x2,x3,x4)
4*(x1+x3)*(x2+x4)*(x2*x4*(x1+x3)+x1*x3*(x2+x4))/((x2*x4*(x1+x3)+(x1*x3)*(x2+x4))*(x1
+x2+x3+x4)+3*(x1+x2)*(x3+x4)*(x1+x3)*(x2+x4));
% importing the input permeability data for RGT
k1=import permeabilitydata3D.txt


% Reshaping the permeability into a row matrix of N elements
Perm1=reshape(permeabilitydata3D,[N,1]);

% Randomizing the permeability values
Perm2=Perm1(randperm(numel(Perm1)));

% reshaping the random Perm2 row matrix into a matrix with size [r,c,r]
k_renorm=reshape(Perm2,[r,c,r]);

% initializing the size of the k_renorm matrix
[nx,ny]=size(k_renorm);
```

```
% defining the new permeability matrix derived from the first step of 3D renormalization
k2=zeros(128,128,128);
% using a for loop to invoke the RGT expression in the first step of 3D renormalization
for iii=1:2:c-1
   for jjj=1:2:r-1
      for kkk=1:2:c-1

k2(iii,jjj,kkk)=0.25*(funn(k1(iii,jjj,kkk),k1(iii+1,jjj,kkk),k1(iii,jjj+1,kkk),k1(iii+1,jjj+1,kkk))+fu
nn(k1(iii,jjj,kkk+1),k1(iii+1,jjj,kkk+1),k1(iii,jjj+1,kkk+1),k1(iii+1,jjj+1,kkk+1))+funn(k1(iii,jjj,k
kk+1),k1(iii+1,jjj,kkk+1),k1(iii,jjj,kkk), k1(iii+1,jjj,kkk))+
funn(k1(iii,jjj+1,kkk+1),k1(iii+1,jjj+1,kkk+1),k1(iii,jjj+1,kkk),k1(iii+1,jjj+1,kkk)));
      end
   end
end
% Removing all elements of the matrix equal to zero
k2=nonzeros(k2);
% Reshaping the final matrix derived from the 3D renormalization first step
k2=reshape(k2,128,128,128);

% defining the new permeability matrix derived from the first step of renormalization
k3=zeros(64,64,64);
% using a for loop to invoke the RGT expression in the second step of 3D renormalization
for iii=1:2:c/2-1
```

```
    for jjj=1:2:r/2-1
        for kkk=1:2:c/2-1

k3(iii,jjj,kkk)=0.25*(funn(k2(iii,jjj,kkk),k2(iii+1,jjj,kkk),k2(iii,jjj+1,kkk),k2(iii+1,jjj+1,kkk))+fu
nn(k2(iii,jjj,kkk+1),k2(iii+1,jjj,kkk+1),k2(iii,jjj+1,kkk+1),k2(iii+1,jjj+1,kkk+1))+funn(k2(iii,jjj,k
kk+1),k2(iii+1,jjj,kkk+1),k2(iii,jjj,kkk),k2(iii+1,jjj,kkk))+funn(k2(iii,jjj+1,kkk+1),k2(iii+1,jjj+1,
kkk+1),k2(iii,jjj+1,kkk),k2(iii+1,jjj+1,kkk)));
            end
    end
end
% Removing all elements of the matrix equal to zero
k3=nonzeros(k3);
% Reshaping the final matrix derived from the 3D renormalization second step
k3=reshape(k3,64,64,64);

% defining the new permeability matrix derived from the second step of 3D renormalization
k4=zeros(32,32,32);
% using a for loop to invoke the RGT expression in the third step of 3D renormalization
for iii=1:2:c/4-1
    for jjj=1:2:r/4-1
        for kkk=1:2:c/4-1

k4(iii,jjj,kkk)=0.25*(funn(k3(iii,jjj,kkk),k3(iii+1,jjj,kkk),k3(iii,jjj+1,kkk),k3(iii+1,jjj+1,kkk))+fu
```

```
nn(k3(iii,jjj,kkk+1),k3(iii+1,jjj,kkk+1),k3(iii,jjj+1,kkk+1),k3(iii+1,jjj+1,kkk+1))+funn(k3(iii,jjj,k
kk+1),k3(iii+1,jjj,kkk+1),k3(iii,jjj,kkk),k3(iii+1,jjj,kkk))+funn(k3(iii,jjj+1,kkk+1),k3(iii+1,jjj+1,
kkk+1),k3(iii,jjj+1,kkk),k3(iii+1,jjj+1,kkk)));
        end
    end
end
% Removing all elements of the matrix equal to zero
k4=nonzeros(k4);
% Reshaping the final matrix derived from the 3D renormalization third step
k4=reshape(k4,32,32,32);

% defining the new permeability matrix derived from the third step of 3D renormalization
k5=zeros(16,16,16);
% using a for loop to invoke the RGT expression in the fourth step of 3D renormalization
for iii=1:2:c/8-1
    for jjj=1:2:r/8-1
        for kkk=1:2:c/8-1

k5(iii,jjj,kkk)=0.25*(funn(k4(iii,jjj,kkk),k4(iii+1,jjj,kkk),k4(iii,jjj+1,kkk),k4(iii+1,jjj+1,kkk))+fu
nn(k4(iii,jjj,kkk+1),k4(iii+1,jjj,kkk+1),k4(iii,jjj+1,kkk+1),k4(iii+1,jjj+1,kkk+1))+funn(k4(iii,jjj,k
kk+1),k4(iii+1,jjj,kkk+1),k4(iii,jjj,kkk),k4(iii+1,jjj,kkk))+funn(k4(iii,jjj+1,kkk+1),k4(iii+1,jjj+1,
kkk+1),k4(iii,jjj+1,kkk),k4(iii+1,jjj+1,kkk)));
        end
```

```
    end
end
% Removing all elements of the matrix equal to zero
k5=nonzeros(k5);
% Reshaping the final matrix derived from the 3D renormalization fourth step
k5=reshape(k5,16,16,16);

% defining the new permeability matrix derived from the fourth step of 3D renormalization
k6=zeros(8,8,8);
% using a for loop to invoke the RGT expression in the fifth step of 3D renormalization
for iii=1:2:c/16-1
    for jjj=1:2:r/16-1
        for kkk=1:2:c/16-1

k6(iii,jjj,kkk)=0.25*(funn(k5(iii,jjj,kkk),k5(iii+1,jjj,kkk),k5(iii,jjj+1,kkk),k5(iii+1,jjj+1,kkk))+fu
nn(k5(iii,jjj,kkk+1),k5(iii+1,jjj,kkk+1),k5(iii,jjj+1,kkk+1),k5(iii+1,jjj+1,kkk+1))+funn(k5(iii,jjj,k
kk+1),k5(iii+1,jjj,kkk+1),k5(iii,jjj,kkk),k5(iii+1,jjj,kkk))+funn(k5(iii,jjj+1,kkk+1),k5(iii+1,jjj+1,
kkk+1),k5(iii,jjj+1,kkk),k5(iii+1,jjj+1,kkk)));
            end
    end
% Removing all elements of the matrix equal to zero
k6=nonzeros(k6);
% Reshaping the final matrix derived from the 3D renormalization fifth step
```

```
k6=reshape(k6,8,8,8);

% defining the new permeability matrix derived from the fifth step of 3D renormalization
k7=zeros(4,4,4);
% using a for loop to invoke the RGT expression in the sixth step of 3D renormalization
for iii=1:2:c/32-1
   for jjj=1:2:r/32-1
      for kkk=1:2:c/32-1

k7(iii,jjj,kkk)=0.25*(funn(k6(iii,jjj,kkk),k6(iii+1,jjj,kkk),k6(iii,jjj+1,kkk),k6(iii+1,jjj+1,kkk))+fu
nn(k6(iii,jjj,kkk+1),k6(iii+1,jjj,kkk+1),k6(iii,jjj+1,kkk+1),k6(iii+1,jjj+1,kkk+1))+funn(k6(iii,jjj,k
kk+1),k6(iii+1,jjj,kkk+1),k6(iii,jjj,kkk),k6(iii+1,jjj,kkk))+funn(k6(iii,jjj+1,kkk+1),k6(iii+1,jjj+1,
kkk+1),k6(iii,jjj+1,kkk),k6(iii+1,jjj+1,kkk)));
         end
   end
end
% Removing all elements of the matrix equal to zero
k7=nonzeros(k7);
% Reshaping the final matrix derived from the 3D renormalization sixth step
k7=reshape(k7,4,4,4);

% defining the new permeability matrix derived from sixth step of renormalization
k8=zeros(2,2,2);
```

```
% using a for loop to invoke the RGT expression in the seventh step of 3D renormalization
for iii=1:2:c/64-1
   for jjj=1:2:r/64-1
      for kkk=1:2:c/64-1

k8(iii,jjj,kkk)=0.25*(funn(k7(iii,jjj,kkk),k7(iii+1,jjj,kkk),k7(iii,jjj+1,kkk),k7(iii+1,jjj+1,kkk))+fu
nn(k7(iii,jjj,kkk+1),k7(iii+1,jjj,kkk+1),k7(iii,jjj+1,kkk+1),k7(iii+1,jjj+1,kkk+1))+funn(k7(iii,jjj,k
kk+1),k7(iii+1,jjj,kkk+1),k7(iii,jjj,kkk),k7(iii+1,jjj,kkk))+funn(k7(iii,jjj+1,kkk+1),k7(iii+1,jjj+1,
kkk+1),k7(iii,jjj+1,kkk),k7(iii+1,jjj+1,kkk)));
         end
   end
end
% Removing all elements of the matrix equal to zero
k8=nonzeros(k8');
% Reshaping the final matrix derived from the 3D renormalization seventh step
k8=reshape(k8,2,2,2);

% defining the new permeability matrix derived from the eighth step of 3D renormalization
k9=zeros(1,1,1);
% using a for loop to invoke the RGT expression in the eighth step of 3D renormalization
for iii=1:2:c/128-1
   for jjj=1:2:r/128-1
      for kkk=1:2:c/128-1
```

```
k9(iii,jjj,kkk)=0.25*(funn(k8(iii,jjj,kkk),k8(iii+1,jjj,kkk),k8(iii,jjj+1,kkk),k8(iii+1,jjj+1,kkk))+fu
nn(k8(iii,jjj,kkk+1),k8(iii+1,jjj,kkk+1),k8(iii,jjj+1,kkk+1),k8(iii+1,jjj+1,kkk+1))+funn(k8(iii,jjj,k
kk+1),k8(iii+1,jjj,kkk+1),k8(iii,jjj,kkk),k8(iii+1,jjj,kkk))+funn(k8(iii,jjj+1,kkk+1),k8(iii+1,jjj+1,
kkk+1),k8(iii,jjj+1,kkk),k8(iii+1,jjj+1,kkk)));
            end
    end
end
% Removing all elements of the matrix equal to zero
k9=nonzeros(k9);

% Writing the effective permeability derived from RGT for each iteration
result(count)=k9;
end

% Exporting the 1000 effective permeability values into an excel file
RenormPerm3D=[result];
xlswrite('RenormPerm3D.xlsx', RenormPerm3D)
```

Appendix C

The MATLAB code developed to estimate the effective permeability using Effective Medium Approximation in ten formations studied here.

```
%This code calculates the effective permeability of a permeability distribution of 2D formations based on the Effective Medium Approximation

% Specifying the minimum and maximum values of permeability
clear all
clc

kmin=6.07488E-14;
kmax=3.17531E-05;

% Generating 1000 permeability values
k=linspace(kmin,kmax,1000);

% Specifying the kg and sigma values of the permeability distribution
kg=1e+9;
sigma=6;

% Defining the log-normal distribution
```

```
fun=@(X) 0.0000000000131./(sqrt(2*pi).*X.*sigma).*exp(-1.*((log(X)-
log(kg))./(sqrt(2)*sigma)).^2);

% Defining the pdf according to the log-normal distribution
f_k=fun(k);

% Initializing the effective permeability
ke=k;

%coordination number for 2D case
zz=4;

% Using a For loop to implement the EMA expression
for i=1:1:1000
   for j=1:1:1000
      EMA(i,j)=((k(j)-ke(i))*f_k(j)/(k(j)+(((zz/2)-1)*ke(i))));
   end
% Initializing the solution of the final EMA formula, including the integration
Sol(i)=abs(trapz(k(:),EMA(i,:)));
end

% Finding the index of the effective permeability
ind=find(Sol==min(Sol));
```

```
% The effective permeability
keff=k(ind);


%This code calculates the effective permeability of a permeability distribution of 3D formations
based on the Effective Medium Approximation

% Specifying the minimum and maximum values of permeability
clear all
clc

kmin=6.07488E-14;
kmax=3.17531E-05;

% Generating 1000 permeability values
k=linspace(kmin,kmax,1000);

% Specifying the kg and sigma values of the permeability distribution
kg=1e+9;
sigma=6;

% Defining the log-normal distribution
```

```
fun=@(X) 0.0000000000131./(sqrt(2*pi).*X.*sigma).*exp(-1.*((log(X)-
log(kg))./(sqrt(2)*sigma)).^2);

% Defining the pdf according to the log-normal distribution
f_k=fun(k);

% Initializing the effective permeability
ke=k;

%coordination number for 3D case
zz=6;

% Using a For loop to implement the EMA expression
for i=1:1:1000
   for j=1:1:1000
      EMA(i,j)=((k(j)-ke(i))*f_k(j)/(k(j)+(((zz/2)-1)*ke(i))));
   end
% Initializing the solution of the final EMA formula, including the integration
Sol(i)=abs(trapz(k(:),EMA(i,:)));
end

% Finding the index of the effective permeability
ind=find(Sol==min(Sol));
```

```
% The effective permeability

keff=k(ind);
```